Proceedings: Fourth International Conference on Recent Advances in Geotechnical Earthquake Engineering
and Soil Dynamics and Symposium in Honor of Professor W.D. Liam Finn
San Diego, California, March 26-31, 2001

RECENT ADVANCES IN SOIL LIQUEFACTION ENGINEERING AND SEISMIC SITE RESPONSE EVALUATION

Seed, R. B.
University of California
Berkeley, California 94720

Cetin, K. O.
Middle East Technical University
Ankara, Turkey

Moss, R. E. S.
Kammerer, A. M.
Wu, J.
Pestana, J. M.
Riemer, M. F.
University of California,
Berkeley, California 94720

ABSTRACT

Over the past decade, major advances have occurred in both understanding and practice with regard to engineering treatment of seismic soil liquefaction and assessment of seismic site response. Seismic soil liquefaction engineering has evolved into a sub-field in its own right, and assessment and treatment of site effects affecting seismic site response has gone from a topic of controversy to a mainstream issue addressed in most modern building codes and addressed in both research and practice. This rapid evolution in the treatment of both liquefaction and site response issues has been pushed by a confluence of lessons and data provided by a series of earthquakes over the past eleven years, as well as by the research and professional/political will engendered by these major seismic events. Although the rate of progress has been laudable, further advances are occurring, and more remains to be done. As we enter a "new millenium", engineers are increasingly well able to deal with important aspects of these two seismic problem areas. This paper will highlight a few major recent and ongoing developments in each of these two important areas of seismic practice, and will offer insights regarding work/research in progress, as well as suggestions regarding further advances needed. The first part of the paper will address soil liquefaction, and the second portion will (briefly) address engineering assessment of seismic site response.

INTRODUCTION

Soil liquefaction is a major cause of damage during earthquakes. "Modern" engineering treatment of liquefaction-related issues evolved initially in the wake of the two devastating earthquakes of 1964, the 1964 Niigata and 1964 Great Alaska Earthquakes, in which seismically-induced liquefaction produced spectacular and devastating effects.

Over the nearly four decades that have followed, significant progress has occurred. Initially, this progress was largely confined to improved ability to assess the likelihood of initiation (or "triggering") of liquefaction in clean, sandy soils. As the years passed, and earthquakes continued to provide lessons and data, researchers and practitioners became increasingly aware of the additional potential problems associated with both silty and gravelly soils, and the issues of post-liquefaction strength and stress-deformation behavior also began to attract increased attention.

Today, the area of "soil liquefaction engineering" is emerging as a semi-mature field of practice in its own right. This area now involves a number of discernable sub-issues or sub-topics, as illustrated schematically in Figure 1. As shown in

Figure 1, the first step in most engineering treatments of soil liquefaction continues to be (1) assessment of "liquefaction potential", or the risk of "triggering" (initiation) of liquefaction. There have been major advances here in recent years, and some of these will be discussed.

Once it is determined that occurrence of liquefaction is a potentially serious risk/hazard, the process next proceeds to assessment of the consequences of the potential liquefaction. This, now, increasingly involves (2) assessment of available post-liquefaction strength and resulting post-liquefaction overall stability (of a site, and/or of a structure or other built facility, etc.). There has been considerable progress in evaluation of post-liquefaction strengths over the past fifteen years. If post-liquefaction stability is found wanting, then deformation/displacement potential is large, and engineered remediation is typically warranted.

If post-liquefaction overall stability is not unacceptable, then attention is next directed towards (3) assessment of anticipated deformations and displacements. This is a very "soft" area of practice, and much remains to be done here with regard to development and calibration/verification of engineering tools and methods. Similarly, relatively little is known regarding
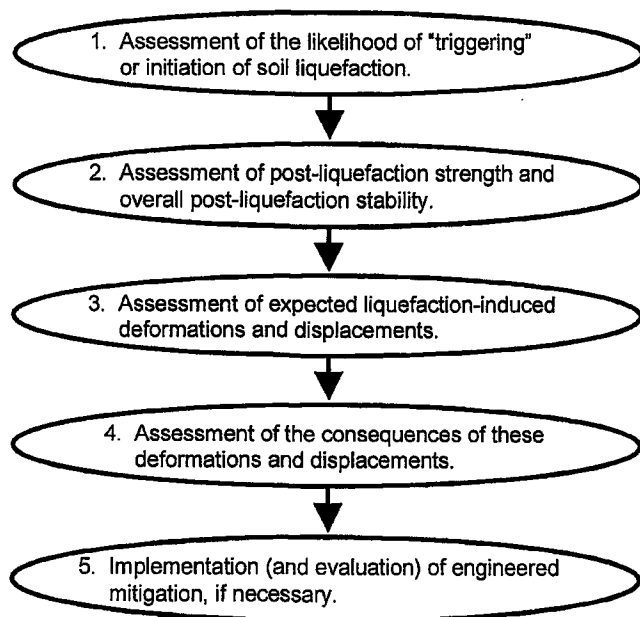
Fig. 1: Key Elements of Soil Liquefaction Engineering

(4) the effects of liquefaction-induced deformations and displacements on the performance of structures and other engineered facilities, and criteria for "acceptable" performance are not well established.

Finally, in cases in which the engineer(s) conclude that satisfactory performance cannot be counted on, (5) engineered mitigation of liquefaction risk is generally warranted. This, too, is a rapidly evolving area, and one rife with potential controversy. Ongoing evolution of new methods for mitigation of liquefaction hazard provides an ever increasing suite of engineering options, but the efficacy and reliability of some of these remain contentious, and accurate and reliable engineering analysis of the improved performance provided by many of these mitigation techniques continues to be difficult.

It is not possible, within the confines of this paper, to fully address all of these issues (a textbook would be required!) Instead, a number of important recent/ongoing advances will be highlighted, and resultant issues and areas of controversy, as well as areas in urgent need of further advances either in practice or understanding, will be noted.

ASSESSMENT OF LIQUEFACTION POTENTIAL

Liquefiable soils:

The first step in engineering assessment of the potential for "triggering" or initiation of soil liquefaction is the determination of whether or not soils of "potentially liquefiable nature" are present at a site. This, in turn, raises the important question regarding which types of soils are potentially vulnerable to soil liquefaction.

It has long been recognized that relatively "clean" sandy soils, with few fines, are potentially vulnerable to seismically-induced liquefaction. There has, however, been significant controversy and confusion regarding the liquefaction potential of silty soils (and silty/clayey soils), and also of coarser, gravelly soils and rockfills.

Coarser, gravelly soils are the easier of the two to discuss, so we will begin there. The cyclic behavior of coarse, gravelly soils differs little from that of "sandy" soils, as Nature has little or no respect for the arbitrary criteria established by the standard #4 sieve. Coarse, gravelly soils are potentially vulnerable to cyclic pore pressure generation and liquefaction. There are now a number of well-documented field cases of liquefaction of coarse, gravelly soils (e.g.: Evans, 1987; Harder, 1988; Hynes, 1988; Andrus, 1994). These soils do, however, often differ in behavior from their finer, sandy brethren in two ways: (1) they can be much more pervious, and so can often rapidly dissipate cyclically generated pore pressures, and (2) due to the mass of their larger particles, the coarse gravelly soils are seldom deposited gently and so do not often occur in the very loose states more often encountered with finer sandy soils. Sandy soils can be very loose to very dense, while the very loose state is uncommon in gravelly deposits and coarser soils.

The apparent drainage advantages of coarse, gravelly soils can be defeated if their drainage potential is circumvented by either; (1) their being surrounded and encapsulated by finer, less pervious materials, (2) if drainage is internally impeded by the presence of finer soils in the void spaces between the coarser particles (it should be noted that the D_{10} particle size, not the mean or D_{50} size, most closely correlates with the permeability of a broadly graded soil mix), or (3) if the layer or stratum of coarse soil is of large dimension, so that the distance over which drainage must occur (rapidly) during an earthquake is large. In these cases, the coarse soils should be considered to be of potentially liquefiable type, and should be evaluated accordingly.

Questions regarding the potential liquefiability of finer, "cohesive" soils (especially "silts") are increasingly common at meetings and professional short courses and seminars. Over the past five years, a group of approximately two dozen leading experts has been attempting to achieve concensus regarding a number of issues involved in the assessment of liquefaction potential. This group, referred to hereafter as the NCEER Working Group, have published many of their consensus findings (or at least near-consensus findings) in the NSF-sponsored workshop summary paper (NCEER, 1997), and additional views are coming in a second paper scheduled for publication this year in the ASCE Journal of Geotechnical and Geoenvironmental Engineering (Youd et al., 2001). The NCEER Working Group addressed this issue, and it was agreed that there was a need to reexamine the "Modified Chinese Criteria" (Finn et al., 1994) for defining the types of
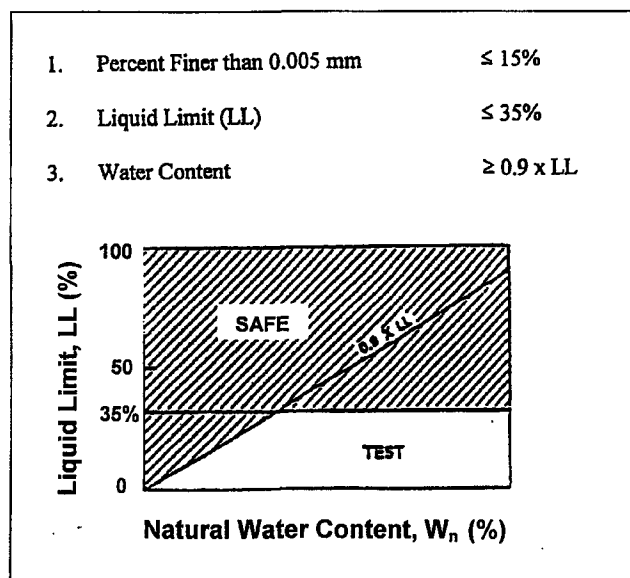
1.	Percent Finer than 0.005 mm	≤ 15%
2.	Liquid Limit (LL)	≤ 35%
3.	Water Content	≥ 0.9 x LL

Fig. 2: Modified Chinese Criteria (After Finn et al., 1994)

fine "cohesive" soils potentially vulnerable to liquefaction, but no improved concensus position could be reached, and more study was warranted.

Some of the confusion here is related to the definition of liquefaction. In this paper, the term "liquefaction" will refer to significant loss of strength and stiffness due to <u>cyclic</u> pore pressure generation, in contrast to "sensitivity" or loss of strength due to monotonic shearing and/or remolding. By making these distinctions, we are able to separately discuss "classical" cyclically-induced liquefaction and the closely-related (but different) phenomenon of strain-softening or sensitivity.

Figure 2 illustrates the "Modified Chinese Criteria" for defining potentially liquefiable soils. According to these criteria, soils are considered to be of potentially liquefiable type and character if: (1) there are less than 15% "clay" fines (based on the Chinese definition of "clay" sizes as less than 0.005 mm), (2) there is a Liquid Limit of LL ≤ 35%, and (3) there is a current in situ water content greater than or equal to 90% of the Liquid Limit.

Andrews and Martin (2000) have re-evaluated the liquefaction field case histories from the database of Seed et al. (1984, 1985), and have transposed the "Modified Chinese Criteria" to U.S. conventions (with clay sizes defined as those less than about 0.002 mm). Their findings are largely summarized in Figure 3. Andrews and Martin recommend that soils with less than about 10% clay fines (< 0.002 mm) and a Liquid Limit (LL) in the minus #40 sieve fraction of less than 32% be considered potentially liquefiable, that soils with more than about 10% clay fines and LL ≥ 32% are unlikely to be susceptible to classic cyclically-induced liquefaction, and that soils intermediate between these criteria should be sampled and tested to assess whether or not they are potentially liquefiable.

This is a step forward, as it somewhat simplifies the previous "Modified Chinese" criteria, and transposes it into terms more familiar to U.S practitioners. We note, however, that there is a common lapse in engineering practice inasmuch as engineers often tend to become distracted by the presence of potentially liquefiable soils, and then often neglect cohesive soils (clays and plastic silts) that are highly "sensitive" and vulnerable to major loss of strength if sheared or remolded. These types of "sensitive" soils often co-exist with potentially liquefiable soils, and can be similarly dangerous in their own right.

Both experimental research and review of liquefaction field case histories show that for soils with sufficient "fines" (particles finer than 0.074 mm, or passing a #200 sieve) to separate the coarser (larger than 0.074 mm) particles, the characteristics of the fines control the potential for cyclically-induced liquefaction. This separation of the coarser particles typically occurs as the fines content exceeds about 12% to 30%, with the precise fines content required being dependent principally on the overall soil gradation and the character of the fines. Well-graded soils have lesser void ratios than uniformly-graded or gap-graded soils, and so require lesser fines contents to separate the coarser particles. Similarly, clay fines carry higher void ratios than silty particles and so are more rapidly effective at over-filling the void space available between the coarser (larger than 0.074mm) particles.

In soils wherein the fines content is sufficient as to separate the coarser particles and control behavior, cyclically-induced soil liquefaction appears to occur primarily in soils where these fines are either non-plastic or are low plasticity silts and/or silty clays (PI ≤ 10 to 12%). In fact, low plasticity or non-plastic silts and silty sands can be among the most dangerous of liquefiable soils, as they not only can cyclically

	Liquid Limit[1] < 32	Liquid Limit ≥ 32
Clay Content[2] < 10%	Susceptible	Further Studies Required *(Considering plastic non-clay sized grains – such as Mica)*
Clay Content[2] ≥ 10%	Further Studies Required *(Considering non-plastic clay sized grains – such as mine and quarry tailings)*	Not Susceptible

Notes:
1. Liquid limit determined by Casagrande-type percussion apparatus.
2. Clay defined as grains finer than 0.002 mm.

Fig. 3: Liquefaction Susceptibility of Silty and Clayey Sands (after Andrews and Martin, 2000)

liquefy; they also "hold their water" well and dissipate excess pore pressures slowly due to their low permeabilities.

Soils with more than about 15% fines, and with fines of "moderate" plasticity (8% ≤ PI ≤ 15%), fall into an uncertain range. These types of soils are usually amenable to reasonably "undisturbed" (e.g.: thin-walled, or better) sampling, however, and so can be tested in the laboratory. It should be remembered to check for "sensitivity" of these cohesive soils as well as for potential cyclic liquefiability.

The criteria of this section do not fully cover all types of liquefiable soils. As an example, a well-studied clayey sand (SC) at a site in the southeastern U.S. has been clearly shown to be potentially susceptible to cyclic liquefaction, despite a clay content on the order of 15 %, and a Plasticity Index of up to 30% (Riemer et al., 1993). This is a highly unusual material, however, as it is an ancient sand that has weathered in place, with the clay largely coating the individual weathered grains, and the overall soil is unusually "loose". Exceptions must be anticipated, and judgement will continue to be necessary in evaluating whether or not specific soils are potentially liquefiable.

Two additional conditions necessary for potential liquefiability are: (1) saturation (or at least near-saturation), and (2) "rapid" (largely "undrained") loading. It should be remembered that phreatic conditions are variable both with seasonal fluctuations and irrigation, and that the rapid cyclic loading induced by seismic excitation represents an ideal loading type.

Assessment of Triggering Potential:

Quantitative assessment of the likelihood of "triggering" or initiation of liquefaction is the necessary first step for most projects involving potential seismically-induced liquefaction. There are two general types of approaches available for this: (1) use of laboratory testing of "undisturbed" samples, and (2) use of empirical relationships based on correlation of observed field behavior with various in-situ "index" tests.

The use of laboratory testing is complicated by difficulties associated with sample disturbance during both sampling and reconsolidation. It is also difficult and expensive to perform high-quality cyclic simple shear testing, and cyclic triaxial testing poorly represents the loading conditions of principal interest for most seismic problems. Both sets of problems can be ameliorated, to some extent, by use of appropriate "frozen" sampling techniques, and subsequent testing in a high quality cyclic simple shear or torsional shear apparatus. The difficulty and cost of these delicate techniques, however, places their use beyond the budget and scope of most engineering studies.

Accordingly, the use of in-situ "index" testing is the dominant approach in common engineering practice. As summarized in the recent state-of-the-art paper (Youd et al., 1997, 2001), four in-situ test methods have now reached a level of sufficient

maturity as to represent viable tools for this purpose, and these are (1) the Standard Penetration Test (SPT), (2) the cone penetration test (CPT), (3) measurement of in-situ shear wave velocity (V_s), and (4) the Becker penetration test (BPT). The oldest, and still the most widely used of these, is the SPT, and this will be the focus of the next section of this paper.

Existing SPT-Based Correlations:

The use of SPT as a tool for evaluation of liquefaction potential first began to evolve in the wake of a pair of devastating earthquakes that occurred in 1964; the 1964 Great Alaskan Earthquake (M = 8+) and the 1964 Niigata Earthquake (M ≈ 7.5), both of which produced significant liquefaction-related damage (e.g.: Kishida, 1966; Koizumi, 1966; Ohsaki, 1966; Seed and Idriss, 1971). Numerous additional researchers have made subsequent progress, and these types of SPT-based methods continue to evolve today.

As discussed by the NCEER Working Group (NCEER, 1997; Youd et al., 2001), one of the most widely accepted and used SPT-based correlations is the "deterministic" relationship proposed by Seed, et al. (1984, 1985). Figure 4 shows this
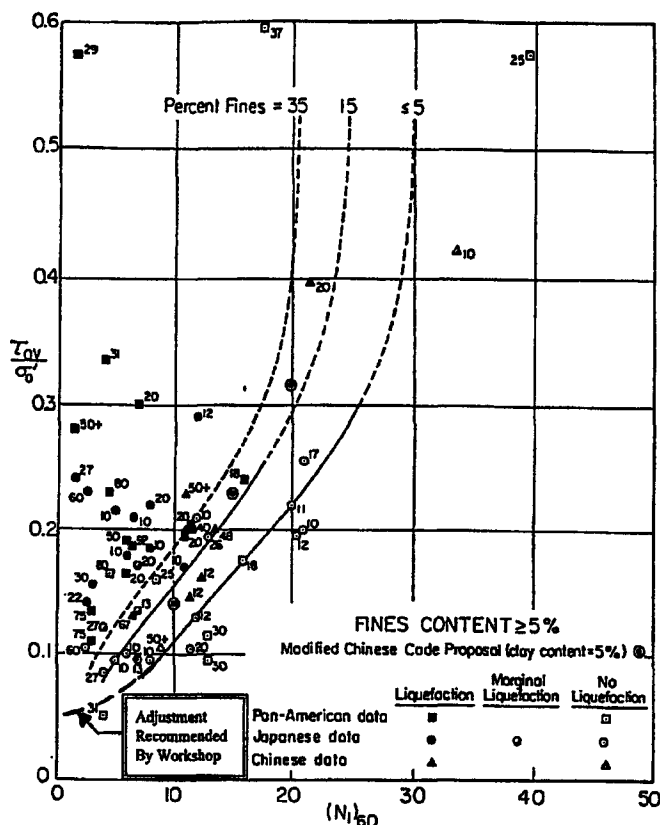

Fig. 4: Correlation Between Equivalent Uniform Cyclic Stress Ratio and SPT $N_{1,60}$-Value for Events of Magnitude M_W≈7.5 for Varying Fines Contents, With Adjustments at Low Cyclic Stress Ratio as Recommended by NCEER Working Group (Modified from Seed, et al., 1986)

relationship, with minor modification at low CSR (as recommended by the NCEER Working Group; NCEER, 1997). This familiar relationship is based on comparison between SPT N-values, corrected for both effective overburden stress and energy, equipment and procedural factors affecting SPT testing (to $N_{1,60}$-values) vs. intensity of cyclic loading, expressed as magnitude-weighted equivalent uniform cyclic stress ratio (CSR_{eq}). The relationship between corrected $N_{1,60}$-values and the intensity of cyclic loading required to trigger liquefaction is also a function of fines content in this relationship, as shown in Figure 4.

Although widely used in practice, this relationship is dated, and does not make use of an increasing body of field case history data from seismic events that have occurred since 1984. It is particularly lacking in data from cases wherein peak ground shaking levels were high (CSR > 0.25), an increasingly common design range in regions of high seismicity. This correlation also has no formal probabilistic basis, and so provides no insight regarding either uncertainty or probability of liquefaction.

Efforts at development of similar, but formally probabilistically-based, correlations have been published by a number of researchers, including Liao et al. (1988, 1998), and more recently Youd and Noble (1997), and Toprak et al. (1999). Figures 5(a) through (c) shows these relationships, expressed as contours of probability of triggering of liquefaction, with the deterministic relationship of Seed et al. from Figure 4 superimposed (dashed lines) for reference. In each of the figures on this page, contours of probability of triggering or initiation of liquefaction for P_L = 5, 20, 50, 80 and 95% are shown.

The probabilistic relationship proposed by Liao et al. employs a larger number of case history data points than were used by Seed et al. (1984), but this larger number of data points is the result of less severe screening of points for data quality, and so includes a number of low quality data. This relationship was developed using the maximum likelihood estimation method for probabilistic regression (binary regression of logistic models). The way the likelihood function was formulated did not permit separate treatment of aleatory and epistemic sources of uncertainty, and so overstates the overall variance or uncertainty of the proposed correlation. This can lead to large levels of over-conservatism at low levels of probability of liquefaction. An additional shortcoming was that Liao et al. sought, but failed to find, a significant impact of fines content on the regressed relationship between SPT penetration resistance and liquefaction resistance, and so developed reliable curves (Figure 5(a)) only for sandy soils with less than 12% fines.

The relationship proposed by Youd and Noble employs a number of field case history data points from earthquakes which have occurred since the earlier relationships were developed, and excludes the most questionable of the data used by Liao et al. The basic methodology employed, maximum likelihood estimation, is the same, however, and as

a result this correlation continues to overstate the overall uncertainty. The effects of fines content were judgmentally prescribed, a priori, in these relationships, and so were not developed as part of the regression. This correlation is applicable to soils of variable fines contents, and so can be employed for both sandy and silty soils. As shown in Figure 5(b), however, uncertainty (or variance) is high.

The relationship proposed by Toprak et al. also employs an enlarged and updated field case history database, and deletes the most questionable of the data used by Liao et al. As with the studies of Youd et al., the basic regression tool was binary regression, and the resulting overall uncertainty is again very large. Similarly, fines corrections and magnitude correlated duration weighting factors were prescribed a priori, rather than regressed from the field case history data, further decreasing model "fit" (and increasing variance and uncertainty).

Overall, these four prior relationships presented in Figures 4 and 5(a) through (c) are all excellent efforts, and are among the best of their types. It is proposed that more can now be achieved, however, using more powerful and flexible probabilistic tools, and taking fullest possible advantage of the currently available field case histories and current knowledge affecting the processing and interpretation of these.

Proposed New SPT-Based Correlations:

This section presents new correlations for assessment of the likelihood of initiation (or "triggering") of soil liquefaction (Cetin, et al., 2000; Seed et al., 2001). These new correlations eliminate several sources of bias intrinsic to previous, similar correlations, and provide greatly reduced overall uncertainty and variance. Figure 5(d) shows the new correlation, with contours of probability of liquefaction again plotted for P_L = 5, 20, 50, 80 and 95%, and plotted to the same scale as the earlier correlations. As shown in this figure, the new correlation provides greatly reduced overall uncertainty. Indeed, the uncertainty is now sufficiently reduced that the principal uncertainty now resides where it belongs; in the engineer's ability to assess suitable CSR and representative $N_{1,60}$ values for design cases.

Key elements in the development of this new correlation were: (1) accumulation of a significantly expanded database of field performance case histories, (2) use of improved knowledge and understanding of factors affecting interpretation of SPT data, (3) incorporation of improved understanding of factors affecting site-specific ground motions (including directivity effects, site-specific response, etc.), (4) use of improved methods for assessment of in-situ cyclic shear stress ratio (CSR), (5) screening of field data case histories on a quality/uncertainty basis, and (6) use of higher-order probabilistic tools (Bayesian Updating). These Bayesian methods (a) allowed for simultaneous use of more descriptive variables than most prior studies, and (b) allowed for appropriate treatment of various contributing sources of aleatory and epistemic uncertainty. The resulting relationships
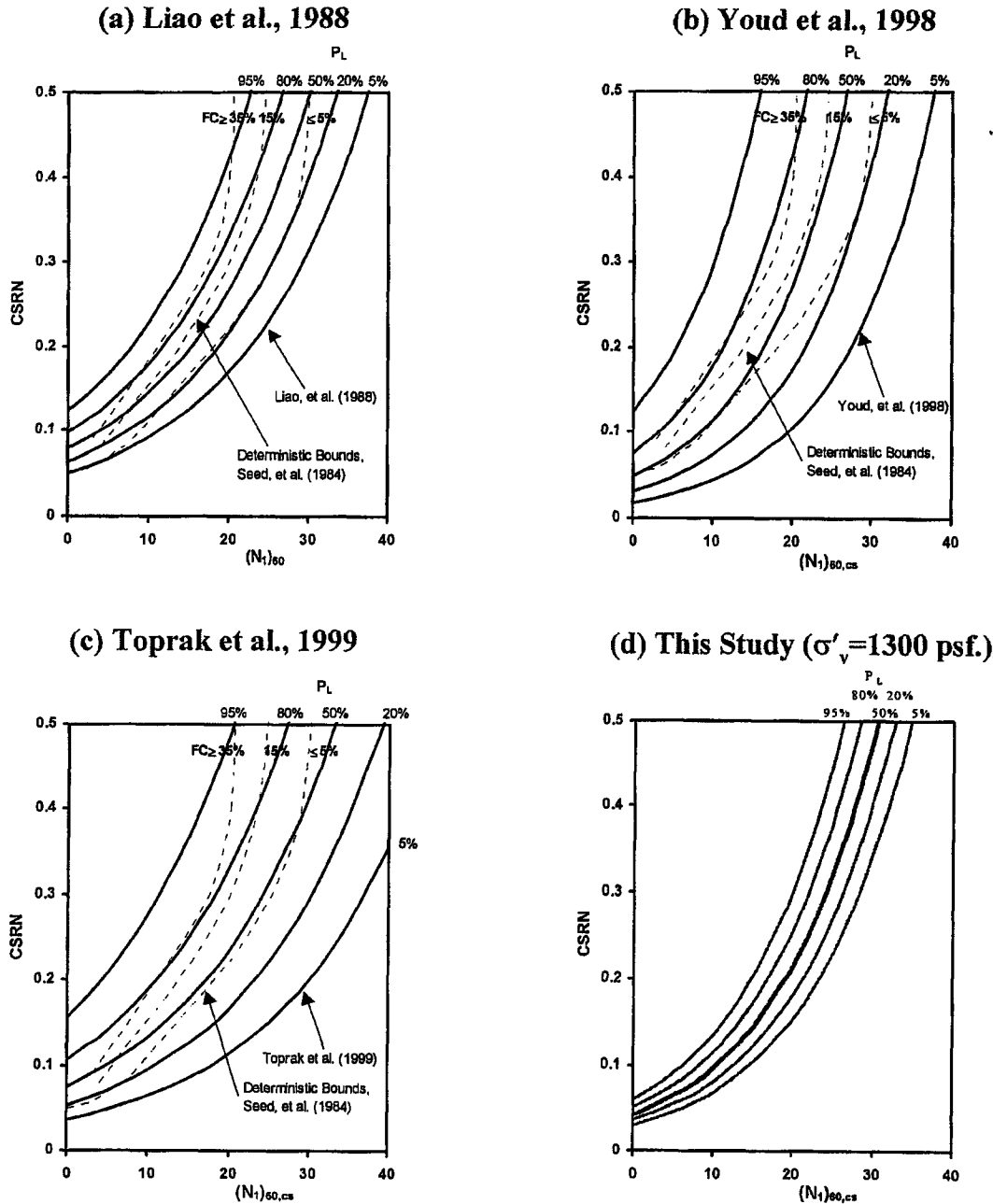
(a) Liao et al., 1988

(b) Youd et al., 1998

(c) Toprak et al., 1999

(d) This Study (σ'_v=1300 psf.)

Fig. 5: Comparison of Best Available Probabilistic Correlations for Evaluation of Liquefaction Potential
(All Plotted for M_w=7.5, σ_v' = 1300 psf, and Fines Content ≤ 5%)

not only provide greatly reduced uncertainty, they also help to resolve a number of corollary issues that have long been difficult and controversial, including: (1) magnitude-correlated duration weighting factors, (2) adjustments for fines content, and (3) corrections for effective overburden stress.

As a starting point, all of the field case histories employed in the correlations shown in Figures 4 and 5(a) through (c) were

obtained and studied. Additional cases were also obtained, including several proprietary data sets. Eventually, approximately 450 liquefaction (and "non-liquefaction") field case histories were evaluated in detail. A formal rating system was established for rating these case histories on the basis of data quality and uncertainty, and standards were established for inclusion of field cases in the final data set used to establish the new correlations. In the end, 201 of the field

case histories were judged to meet these new and higher standards, and were employed in the final development of the proposed new correlations.

A significant improvement over previous efforts was the improved evaluation of peak horizontal ground acceleration at each earthquake field case history site. Specific details are provided by Cetin et al. (2001). Significant improvements here were principally due to improved understanding and treatment of issues such as (a) directivity effects, (b) effects of site conditions on response, (c) improved attenuation relationships, and (d) availability of strong motion records from recent (and well-instrumented) major earthquakes. In these studies, peak horizontal ground acceleration (a_{max}) was taken as the geometric mean of two recorded orthogonal horizontal components. Whenever possible, attenuation relationships were calibrated on an earthquake-specific basis, based on local strong ground motion records, significantly reducing uncertainties. For all cases wherein sufficiently detailed data and suitable nearby recorded ground motions were available, site-specific site response analyses were performed. In all cases, both local site effects and rupture-mechanism-dependent potential directivity effects were also considered.

A second major improvement was better estimation of in-situ CSR within the critical stratum for each of the field case histories. All of the previous studies described so far used the "simplified" method of Seed and Idriss (1971) to estimate CSR at depth (within the critical soil stratum) as

$$CSR_{peak} = \left(\frac{a_{max}}{g}\right) \cdot \left(\frac{\sigma_v}{\sigma'_v}\right) \cdot (r_d) \qquad \text{(Eq. 1)}$$

where
- a_{max} = the peak horizontal ground surface acceleration,
- g = the acceleration of gravity,
- σ_v = total vertical stress,
- σ'_v = effective vertical stress, and
- r_d = the nonlinear shear mass participation factor.

The original r_d values proposed by Seed and Idriss (1971) are shown by the heavy lines in Figure 6(a). These are the values used in the previous studies by Seed et al. (1984), Liao et al. (1988, 1998), Youd et al. (1997), and Toprak et al. (1999).

Recognition that r_d is nonlinearly dependent upon a suite of factors led to studies by Cetin and Seed (2000) to develop improved correlations for estimation of r_d. The numerous light gray lines in Figures 6(a) and (b) show the results of 2,153 seismic site response analyses performed to assess the variation of r_d over ranges of (1) site conditions, and (2) ground motion excitation characteristics. The mean and ± 1 standard deviation values for these 2,153 analyses are shown by the heavy lines in Figure 6(b). As shown in Figures 6(a) and (b), the earlier r_d proposal of Seed and Idriss (1971) understates the variance, and provides biased (generally high) estimates of r_d at depths of between 10 and 50 feet (3 to 15 m.) Unfortunately, it is in this depth range that the critical
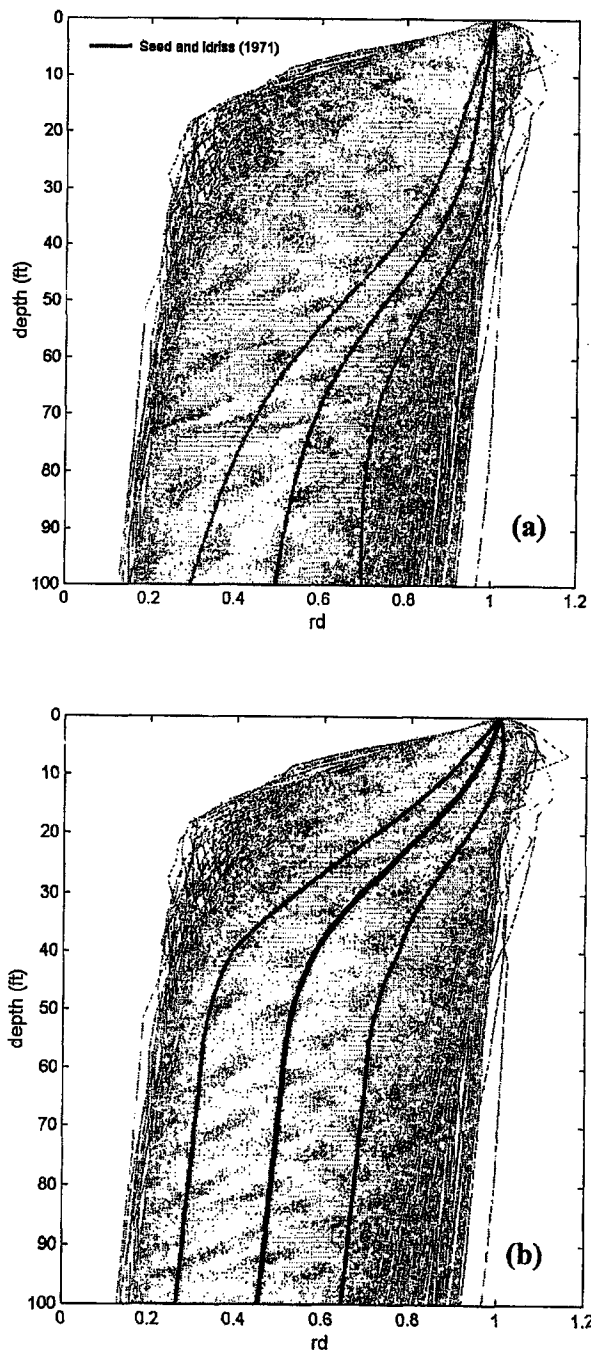

Fig. 6: R_d Results from Response Analyses for 2,153 Combinations of Site Conditions and Ground Motions, Superimposed with Heavier Lines Showing (a) the Earlier Recommendations of Seed and Idriss (1971), and (b) the Mean and ± 1 Standard Deviation Values for the 2,153 Cases Analyzed (After Cetin and Seed, 2000).

d < 65 ft:

$$r_d(d, M_w, a_{max}, V_{s,40'}^*) = \frac{\left[1 + \dfrac{-23.013 - 2.949 \cdot a_{max} + 0.999 \cdot M_w + 0.016 \cdot V_{s,40'}^*}{16.258 + 0.201 \cdot e^{0.104 \cdot (-d + 0.0785 \cdot V_{s,40'}^* + 24.888)}}\right]}{\left[1 + \dfrac{-23.013 - 2.949 \cdot a_{max} + 0.999 \cdot M_w + 0.016 \cdot V_{s,40'}^*}{16.258 + 0.201 \cdot e^{0.104 \cdot (0.0785 \cdot V_{s,40'}^* + 24.888)}}\right]} \pm \sigma_{\varepsilon_{r_d}} \qquad \textbf{(Eq 2)}$$

d ≥ 65 ft:

$$r_d(d, M_w, a_{max}, V_{s,40'}^*) = \frac{\left[1 + \dfrac{-23.013 - 2.949 \cdot a_{max} + 0.999 \cdot M_w + 0.016 \cdot V_{s,40'}^*}{16.258 + 0.201 \cdot e^{0.104 \cdot (-65 + 0.0785 \cdot V_{s,40'}^* + 24.888)}}\right]}{\left[1 + \dfrac{-23.013 - 2.949 \cdot a_{max} + 0.999 \cdot M_w + 0.016 \cdot V_{s,40'}^*}{16.258 + 0.201 \cdot e^{0.104 \cdot (0.0785 \cdot V_{s,40'}^* + 24.888)}}\right]} - 0.0014 \cdot (d - 65) \pm \sigma_{\varepsilon_{r_d}}$$

where

$$\sigma_{\varepsilon_{r_d}}(d) = d^{0.850} \cdot 0.0072 \quad \text{[for d < 40 ft], and}$$

$$\sigma_{\varepsilon_{r_d}}(d) = 40^{0.850} \cdot 0.0072 \quad \text{[for d ≥ 40 ft]}$$

soil strata for most of the important liquefaction (and non-liquefaction) earthquake field case histories occur. This, in turn, creates some degree of corresponding bias in relationships developed on this basis.

Cetin and Seed (2000, 2001) propose a new, empirical basis for estimation of r_d as a function of; (1) depth, (2) earthquake magnitude, (3) intensity of shaking, and (4) site stiffness (as expressed in Equation 2).

Figure 7 shows the values of r_d from the 2,153 site response analyses performed as part of these studies sub-divided into 12 "bins" as a function of peak ground surface acceleration (a_{max}), site stiffness ($V_{s,40ft}$), earthquake magnitude (M_w), and depth (d). [$V_{s,40ft}$ is the "average" shear wave velocity over the top 40 feet of a site (in units of ft./sec.), taken as 40 feet divided by the shear wave travel time in traversing this 40 feet.] Superimposed on each figure are the mean and ± 1 standard deviation values central to each "bin" from Equation 2. Either Equation 2, or Figure 7, can be used to derive improved (and statistically unbiased) estimates of r_d.

It is noted, however, that in-situ CSR (and r_d) can "jump" or transition irregularly within a specific soil profile, especially near sharp transitions between "soft" and "stiff" strata, and that CSR (and r_d) are also a function of the interaction between a site and each specific excitation motion. Accordingly, the best means of estimation of in-situ CSR within any given stratum is to directly calculate CSR by means of appropriate site-specific, and event-specific, seismic site response analyses, when this is feasible. As the new correlations were developed using both directly-calculated r_d values (from site response analyses) as well as r_d values from the statistically

unbiased correlation of Equation 2, there is no intrinsic a priori bias associated with either approach.

In these new correlations, in-situ cyclic stress ratio (CSR) is taken as the "equivalent uniform CSR" equal to 65% of the single (one-time) peak CSR (from Equation 1) as

$$CSR_{eq} = (0.65) \cdot CSR_{peak} \qquad \text{(Eq. 3)}$$

In-situ CSR_{eq} was evaluated directly, based on performance of full seismic site response analyses (using SHAKE 90; Idriss and Sun, 1992), for cases where (a) sufficient sub-surface data was available, and (b) where suitable "input" motions could be developed from nearby strong ground motion records. For cases wherein full seismic site response analyses were not performed, CSR_{eq} was evaluated using the estimated a_{max} and Equations 1 and 2. In addition to the best estimates of CSR_{eq}, the variance or uncertainty of these estimates (due to all contributing sources of uncertainty) was also assessed (Cetin et al., 2001).

At each case history site, the critical stratum was identified as the stratum most susceptible to triggering of liquefaction. When possible, collected surface boil materials were also considered, but problems associated with mixing and segregation during transport, and recognition that liquefaction of underlying strata can result in transport of overlying soils to the surface through boils, limited the usefulness of some of this data.
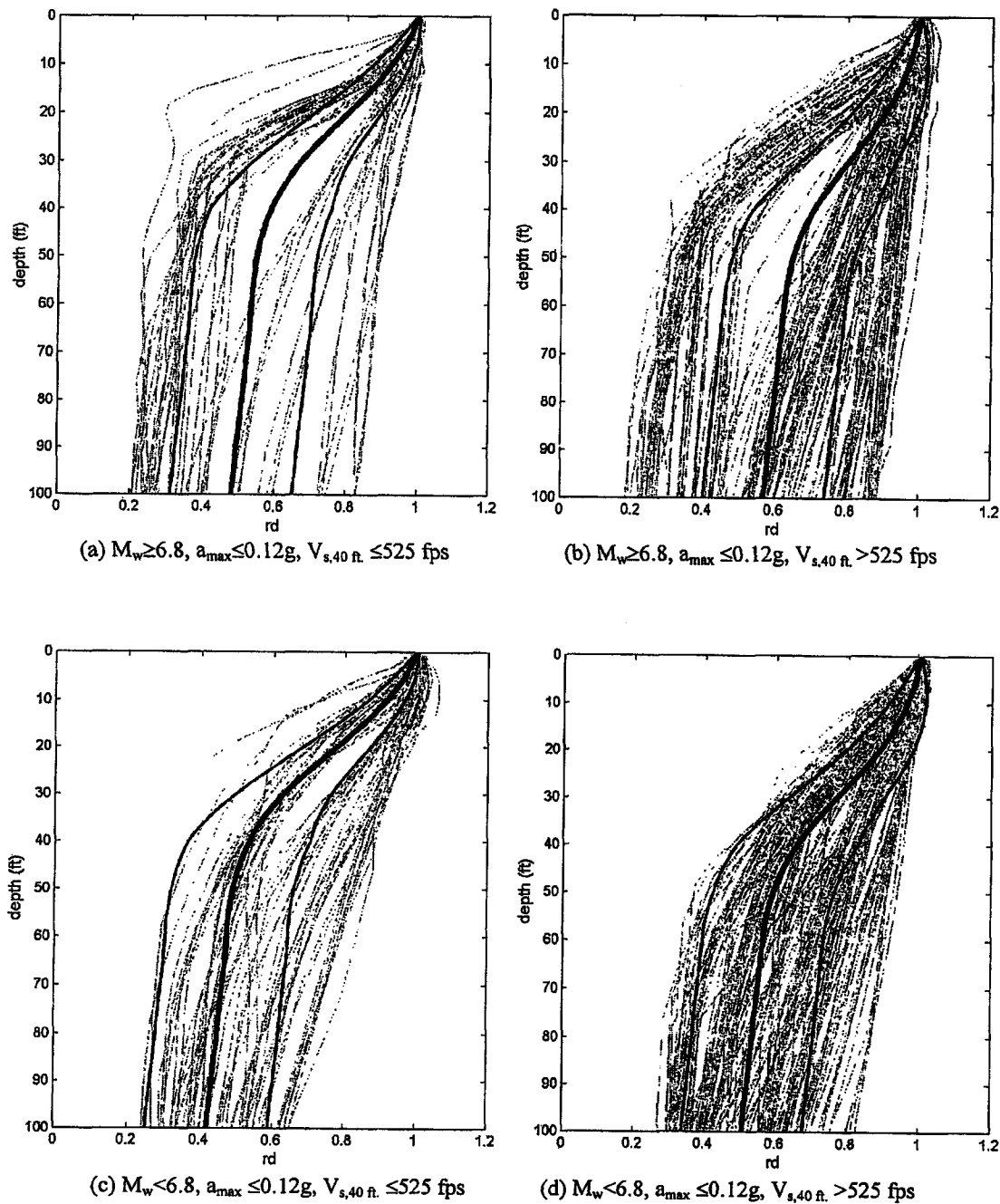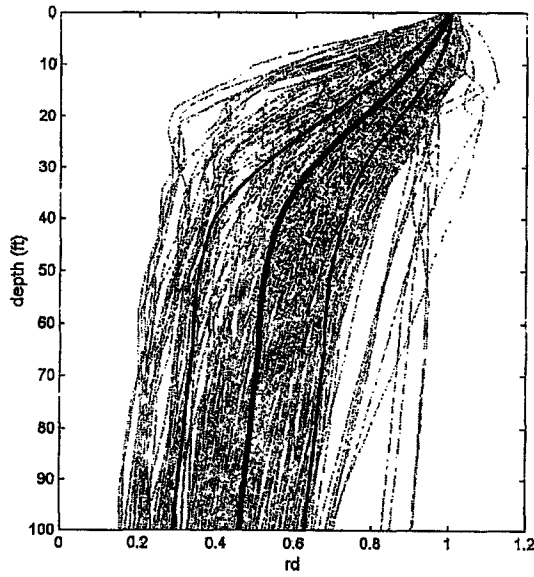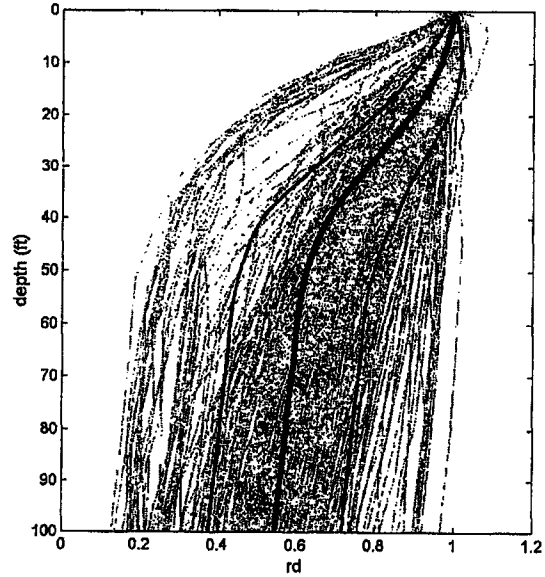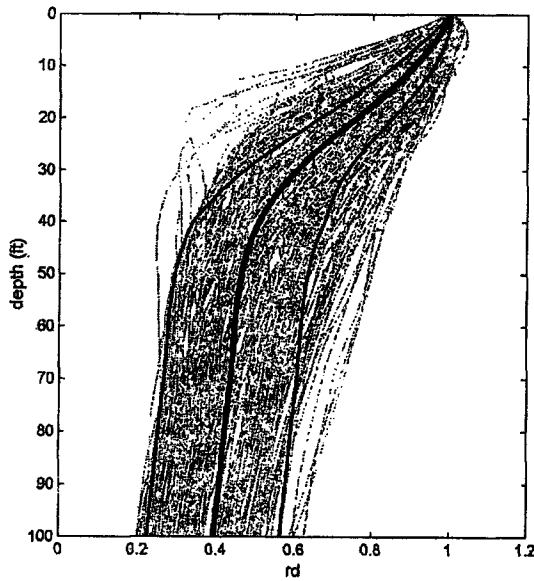
(a) $M_w \geq 6.8$, $a_{max} \leq 0.12g$, $V_{s,40\,ft.} \leq 525$ fps

(b) $M_w \geq 6.8$, $a_{max} \leq 0.12g$, $V_{s,40\,ft.} > 525$ fps

(c) $M_w < 6.8$, $a_{max} \leq 0.12g$, $V_{s,40\,ft.} \leq 525$ fps

(d) $M_w < 6.8$, $a_{max} \leq 0.12g$, $V_{s,40\,ft.} > 525$ fps

Fig. 7: R_d Results for Various "Bins" Superimposed with the Predictions (Mean and Mean ±1σ) Based on Bin Mean Values of $V_{s,40\,ft}$, M_w, and a_{max} (continued...)
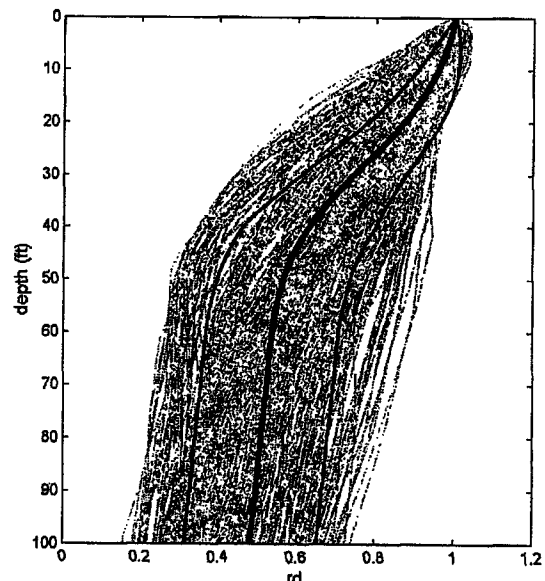
(e) $M_w \geq 6.8$, $0.12 < a_{max} \leq 0.23g$, $V_{s,40 ft.} \leq 525$ fps   (f) $M_w \geq 6.8$, $0.12 < a_{max} \leq 0.23g$, $V_{s,40 ft.} > 525$ fps
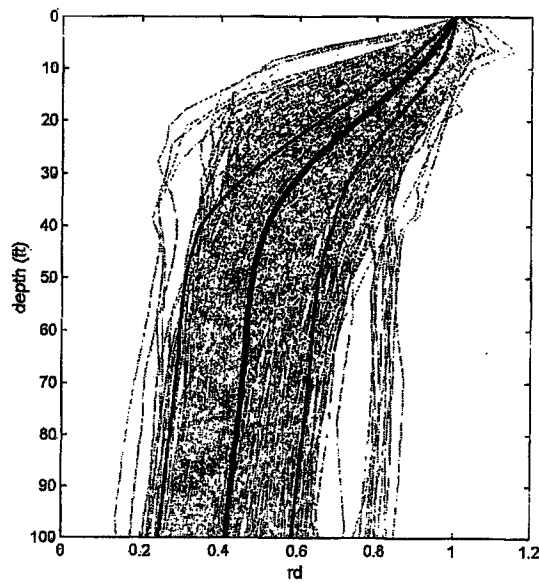
(g) $M_w < 6.8$, $0.12 < a_{max} \leq 0.23g$, $V_{s,40 ft.} \leq 525$ fps   (h) $M_w < 6.8$, $0.12 < a_{max} \leq 0.23g$, $V_{s,40 ft.} > 525$ fps
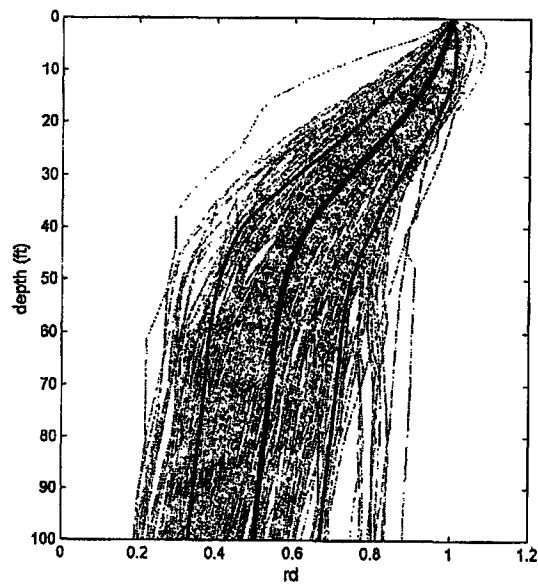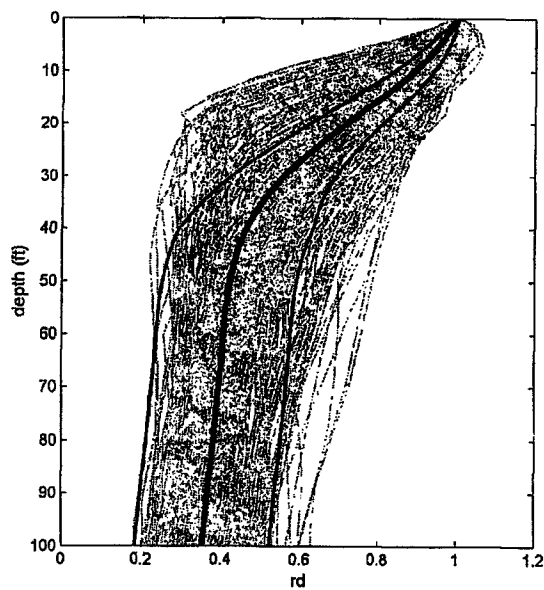
Fig. 7: R_d Results for Various "Bins" Superimposed with the Predictions (Mean and Mean $\pm 1\sigma$) Based on Bin Mean Values of $V_{s,40 ft}$, M_w, and a_{max} (continued...)
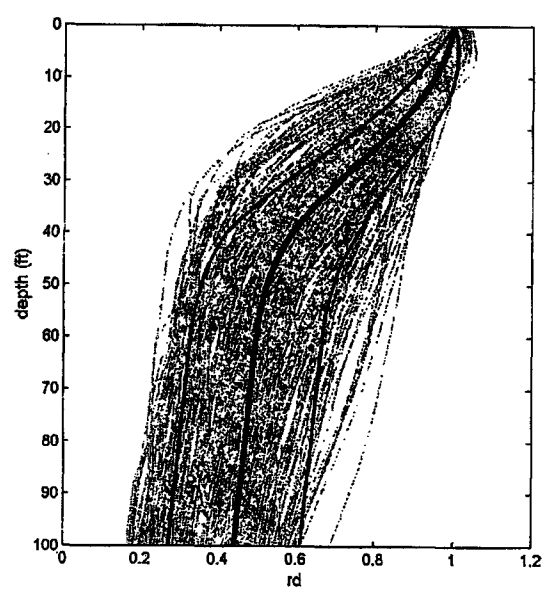
(i) $M_w \geq 6.8$, $0.23 < a_{max}$, $V_{s,40\,ft.} \leq 525$ fps

(j) $M_w \geq 6.8$, $0.23 < a_{max}$, $V_{s,40\,ft.} > 525$ fps

(k) $M_w < 6.8$, $0.23 < a_{max}$, $V_{s,40\,ft.} \leq 525$ fps

(l) $M_w < 6.8$, $0.23 < a_{max}$, $V_{s,40\,ft.} > 525$ fps

Fig. 7: R_d Results for Various "Bins" Superimposed with the Predictions (Mean and Mean $\pm 1\sigma$) Based on Bin Mean Values of $V_{s,40\,ft}$, M_w, and a_{max}

The $N_{1,60}$-values employed were "truncated mean values" within the critical stratum. Measured N-values (from one or more points) within a critical stratum were corrected for overburden, energy, equipment, and procedural effects to $N_{1,60}$ values, and were then plotted vs. elevation. In many cases, a given soil stratum would be found to contain an identifiable sub-stratum (based on a group of localized low $N_{1,60}$-values) that was significantly more critical than the rest of the stratum. In such cases, the <u>sub</u>-stratum was taken as the "critical stratum". Occasional high values, not apparently representative of the general characteristics of the critical stratum, were considered "non-representative" and were deleted in a number of the cases. Similarly, though less often, very low $N_{1,60}$ values (very much lower than the apparent main body of the stratum, and often associated with locally high fines content) were similarly deleted. The remaining, corrected $N_{1,60}$ values were then used to evaluate both the mean of $N_{1,60}$ within the critical stratum, and the variance in $N_{1,60}$.

For those cases wherein the critical stratum had only one single useful $N_{1,60}$-value, the coefficient of variation was taken as 20%; a value typical of the larger variances among the cases with multiple $N_{1,60}$ values within the critical stratum (reflecting the increased uncertainty due to lack of data when only a single value was available).

All N-values were corrected for overburden effects (to the hypothetical value, N_1, that "would" have been measured if the effective overburden stress at the depth of the SPT had been 1 atmosphere) [1 atm. $\approx$ 2,000 lb/ft^2 $\approx$ 1 kg/cm^2 $\approx$ 14.7 lb/in^2 $\approx$ 101 kPa] as

$$N_1 = N \cdot C_N \qquad \text{(Eq. 4(a))}$$

where C_N is taken (after Liao and Whitman, 1986) as

$$C_N = \left(\frac{1}{\sigma'_v} \right)^{0.5} \qquad \text{(Eq. 4(b))}$$

where σ'_v is the actual effective overburden stress at the depth of the SPT in atmospheres.

The resulting N_1 values were then further corrected for energy, equipment, and procedural effects to <u>fully</u> standardized $N_{1,60}$ values as

$$N_{1,60} = N_1 \cdot C_R \cdot C_S \cdot C_B \cdot C_E \qquad \text{(Eq. 5)}$$

where C_R = correction for "short" rod length,
          C_S = correction for non-standardized sampler configuration,
          C_B = correction for borehole diameter, and
          C_E = correction for hammer energy efficiency.

The corrections for C_R, C_S, C_B and C_E employed correspond largely to those recommended by the NCEER Working Group (NCEER, 1997).

Table 1 summarizes the correction factors used in these studies. The correction for "short" rod length between the driving hammer and the penetrating sampler was taken as a nonlinear "curve" (Figure 8), rather than the incremental values of the NCEER Workshop recommendations, but the two agree well at all NCEER mid-increments of length.

C_S was applied in cases wherein a "nonstandard" (though very common) SPT sampler was used in which the sampler had an internal space for sample liner rings, but the rings were not used. This results in an "indented" interior liner annulus of enlarged diameter, and reduces friction between the sample and the interior of the sampler, resulting in reduced overall penetration resistance (Seed et al., 1984 and 1985). The reduction in penetration resistance is on the order of ~10 % in loose soils (N_1<10 blows/ft), and ~30 % in very dense soils (N_1>30 blows/ft), so C_S varied from 1.1 to 1.3 over this range.

Borehole diameter corrections (C_B) were as recommended in the NCEER Workshop Proceedings.

Corrections for hammer energy (C_E), which were often significant, were largely as recommended by the NCEER Working Group, except in those cases where better hammer/system-specific information was available. Cases where better information was available included cases where either direct energy measurements were made during driving of the SPT sampler, or where the hammer and the raising/dropping system (and the operator, when appropriate) had been reliably calibrated by means of direct driving energy measurements.

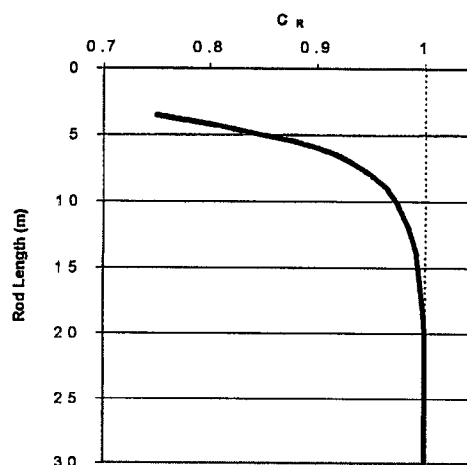Within the Bayesian updating analyses, which were performed using a modified version of the program BUMP (Geyskins

Fig. 8: Recommended C_R Values (rod length from point of hammer impact to tip of sampler).

Table 1: Recommended Corrections for SPT Equipment, Energy and Procedures

C_R	(See Fig. 8 for Rod Length Correction Factors)
C_S	For samplers with an indented space for interior liners, but with liners omitted during sampling, $$C_S = 1 + \frac{N_{1,60}}{10} \qquad \text{(Eq. T-1)}$$ With limits as $1.10 \leq C_S \leq 1.30$
C_B	<table><tr><td>Borehole diameter</td><td>Correction (C_B)</td></tr><tr><td>65 to 115 mm</td><td>1.00</td></tr><tr><td>150 mm</td><td>1.05</td></tr><tr><td>200 mm</td><td>1.15</td></tr></table>
C_E	$C_E = \dfrac{ER}{60\%}$ where ER (efficiency ratio) is the fraction or percentage of the theoretical SPT impact hammer energy actually transmitted to the sampler, expressed as % (Eq. T-2) • The best approach is to directly measure the impact energy transmitted with each blow. When available, direct energy measurements were employed. • The next best approach is to use a hammer and mechanical hammer release system that has been previously calibrated based on direct energy measurements. • Otherwise, ER must be estimated. For good field procedures, equipment and monitoring, the following guidelines are suggested: <table><tr><td>Equipment</td><td>Approximate ER (see Note 3)</td><td>C_E (see Note 3)</td></tr><tr><td>-Safety Hammer[1]</td><td>0.4 to 0.75</td><td>0.7 to 1.2</td></tr><tr><td>-Donut Hammer[1]</td><td>0.3 to 0.6</td><td>0.5 to 1.0</td></tr><tr><td>-Donut Hammer[2]</td><td>0.7 to 0.85</td><td>1.1 to 1.4</td></tr><tr><td>-Automatic-Trip Hammer (Donut or Safety Type)</td><td>0.5 to 0.8</td><td>0.8 to 1.4</td></tr></table> • For lesser quality fieldwork (e.g. irregular hammer drop distance, excessive sliding friction of hammer on rods, wet or worn rope on cathead, etc.) further judgmental adjustments are needed.

Notes: (1) Based on rope and cathead system, two turns of rope around cathead, "normal" release (not the Japanese "throw"), and rope not wet or excessively worn.
(2) Rope and cathead with special Japanese "throw" release. (See also Note 4.)
(3) For the ranges shown, values roughly central to the mid-third of the range are more common than outlying values, but ER and C_E can be even more highly variable than the ranges shown if equipment and/or monitoring and procedures are not good.
(4) Common Japanese SPT practice requires additional corrections for borehole diameter and for frequency of SPT hammer blows. For "typical" Japanese practice with rope and cathead, donut hammer, and the Japanese "throw" release, the overall product of $C_B \times C_E$ is typically in the range of 1.0 to 1.3.

et al., 1993), all field case history data were modeled not as "points", but rather as distributions, with variances in both CSR and $N_{1,60}$ These regression-type analyses were simultaneously applied to a number of contributing variables, and the resulting proposed correlations are illustrated in Figures 5(d) and 7 through 12, and are expressed in Equations 6 through 12.

Figure 9(a) shows the proposed probabilistic relationship between duration-corrected equivalent uniform cyclic stress ratio (CSR_{eq}), and fines-corrected penetration resistances ($N_{1,60,cs}$), with the correlations as well as all field data shown normalized to an effective overburden stress of $\sigma'_v = 0.65$ atm. (1,300 lb/ft^2). The contours shown (solid lines) are for probabilities of liquefaction of P_L=5%, 20%, 50%, 80%, and 95%. All "data points" shown represent median values, also corrected for duration and fines. These are superposed (dashed lines) with the relationship proposed by Seed et al. (1984) for reference.

As shown in this figure, the "clean sand" (Fines Content ≤ 5%) line of Seed et al. (1984) appears to corresponds roughly to P_L≈50%. This is not the case, however, as the Seed et al. (1984) line was based on biased values of CSR (as a result of biased r_d at shallow depths, as discussed earlier.) The new correlation uses actual event-specific seismic site response analyses for evaluation of in situ CSR in 53 of the back-analyzed case histories, and the new (and statistically unbiased) empirical estimation of r_d (as a function of level of shaking, site stiffness, and earthquake magnitude) as presented in Equation 2 and Figure 7 (Cetin and Seed, 2000) for the remaining 148 case histories. The new (improved) estimates of in-situ CSR tend to be slightly lower, typically on the order of ~ 5 to 15% lower, at the shallow depths that are critical in most of the case histories. Accordingly, the CSR's of the new correlation are also, correspondingly, lower by about 5 to 15%, and a fully direct comparison between the new correlation and the earlier recommendations of Seed et al. (1984) cannot be made.

It should be noted that the use of slightly biased (high) values of r_d was not problematic in the earlier correlation of Seed et al. (1984), so long as the same biased (r_d) basis was employed in forward application of this correlation to field engineering works. It was a slight problem, however, when forward applications involved direct, response-based calculation of in-situ CSR, as often occurs on major analyses of dams, etc.

It was Seed's intent that the recommended (1984) boundary should represent approximately a 10 to 15% probability of liquefaction, and with allowance for the "shift" in (improved) evaluation of CSR, the 1984 deterministic relationship for clean sands (<5% fines) does correspond to approximately P_L ≈ 10 to 30%, except at very high CSR (CSR > 0.3), a range in which data was previously scarce.

Also shown in Figure 9(a) is the boundary curve proposed by Yoshimi et al. (1994), based on high quality cyclic testing of frozen samples of alluvial sandy soils. The line of Yoshimi et

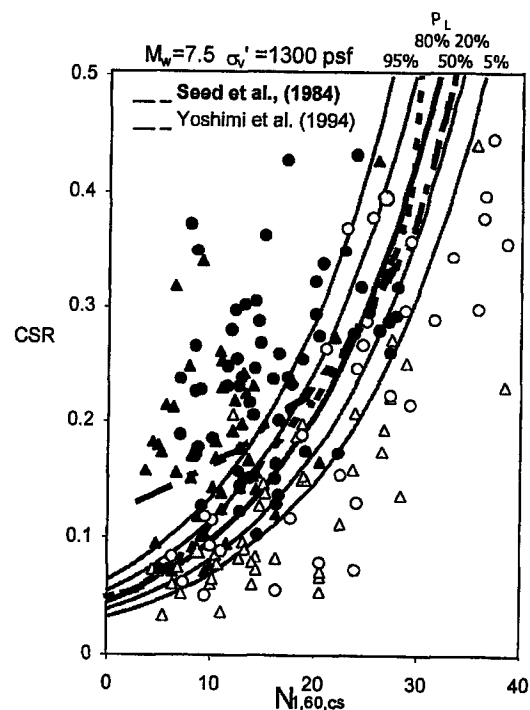

Fig. 9(a): Recommended Probabilistic SPT-Based Liquefaction Triggering Correlation (for M_w=7.5 and σ_v'=0.65 atm), and the Relationship for "Clean Sands" Proposed by Seed et al. (1984)
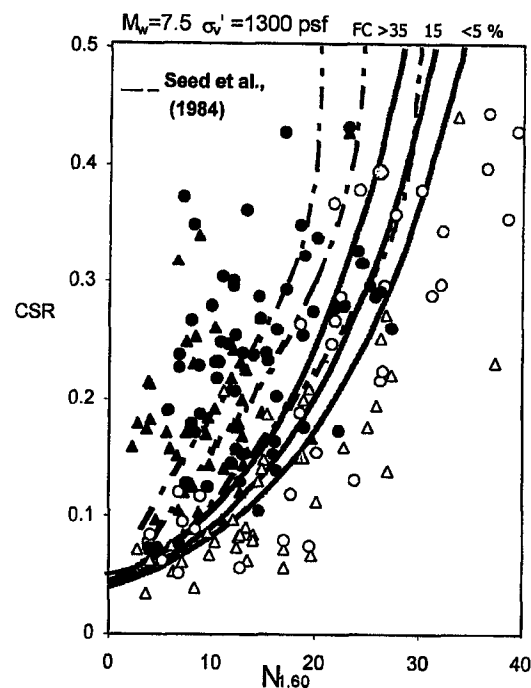

Fig. 9(b): Recommended "Deterministic" SPT-Based Liquefaction Triggering Correlation (for M_w=7.5 and σ_v'=0.65 atm), with Adjustments for Fines Content Shown

al. is arguably unconservatively biased at very low densities (low N-values) as these loose samples densified during laboratory thawing and reconsolidation. Their testing provides potentially valuable insight, however, at high N-values where reconsolidation densification was not significant. In this range, the new proposed correlation provides slightly better agreement with the test data than does the earlier relationship proposed by Seed et al. (1984).

The new correlation is also presented in Figure 5(d), where it can be compared directly with the earlier probabilistic relationships of Figures 5(a) through (c). Here, again, the new correlation is normalized to $\sigma'_v = 0.65$ atm. in order to be fully compatible with the basis of the other relationships shown. As shown in this figure, the new correlation provides a tremendous reduction in overall uncertainty (or variance).

Adjustments for Fines Content:

The new (probabilistic) boundary curve for $P_L = 20\%$ (again normalized to an effective overburden stress of $\sigma'_v = 0.65$ atm.) represents a suitable basis for illustration of the new correlation's <u>regressed</u> correction for the effects of fines content, as shown in Figure 9(b). In this figure, both the correlation as well as the mean values (CSR and $N_{1,60}$) of the field case history data are shown not corrected for fines (this time the N-value axis is <u>not</u> corrected for fines content effects, so that the ($P_L=20\%$) boundary curves are, instead, offset to account for varying fines content.) In this figure, the earlier correlation proposed by Seed et al. (1984) is also shown (with dashed lines) for approximate comparison.

In these current studies, based on the overall (regressed) correlation, the energy- and procedure- and overburden-corrected N-values ($N_{1,60}$) are further corrected for fines content as

$$N_{1,60,CS} = N_{1,60} \cdot C_{FINES} \qquad \text{(Eq. 6)}$$

where the fines correction was "regressed" as a part of the Bayesian updating analyses. The fines correction is equal to zero for fines contents of $FC \leq 5\%$, and reaches a maximum (limiting) value for $FC \geq 35\%$. As illustrated in Figure 9(b), the maximum fines correction results in an increase of N-values of about +6 blows/ft. (at $FC \geq 35\%$, and high CSR). As illustrated in this figure, this maximum fines correction is somewhat smaller than the earlier maximum correction of +9.5 blows/ft proposed by Seed et al. (1984).

The regressed relationship for C_{FINES} is

$$C_{FINES} = \left(1 + 0.004 \cdot FC\right) + 0.05 \cdot \left(\frac{FC}{N_{1,60}}\right)$$

$$\text{lim: } FC \geq 5\% \text{ and } FC \leq 35\% \qquad \text{(Eq. 7)}$$

where FC = percent fines content (percent by dry weight finer than 0.074mm), expressed as an integer (e.g. 15% fines is expressed as 15), and $N_{1,60}$ is in units of blows/ft.

Magnitude-Correlated Duration Weighting:

Both the probabilistic and "deterministic" (based on $P_L=20\%$) new correlations presented in Figures 9(a) and (b) are based on the correction of "equivalent uniform cyclic stress ratio" (CSR_{eq}) for duration (or number of equivalent cycles) to CSRN, representing the equivalent CSR for a duration typical of an "average" event of $M_W = 7.5$. This was done by means of a magnitude-correlated duration weighting factor (DWF_M) as

$$CSRN = CSR_{eq,M=7.5} = CSR_{eq} / DWF_M \qquad \text{(Eq. 8)}$$

This duration weighting factor has been somewhat controversial, and has been developed by a variety of different approaches (using cyclic laboratory testing and/or field case history data) by a number of investigators. Figure 10(a) summarizes a number of recommendations, and shows (shaded zone) the recommendations of the NCEER Working Group (NCEER, 1997). In these current studies, this important and controversial factor could be regressed as a part of the Bayesian Updating analyses. Moreover, the factor (DWF_M) could also be investigated for possible dependence on density (correlation with $N_{1,60}$). Figures 10(a) and (b) show the resulting values of DWF_M, as a function of varying corrected $N_{1,60}$-values. As shown in Figure 10(b), the dependence on density, or $N_{1,60}$-values, was found to be relatively minor.

The duration weighting factors shown in Figures 10(a) and (b) fall slightly below those recommended by the NCEER Working group, and slightly above (but very close to) recent recommendations of Idriss (2000). Idriss' recommendations are based on a judgmental combination of interpretation of high-quality cyclic simple shear laboratory test data and empirical assessment of "equivalent" numbers of cycles from recorded strong motion time histories, and are the only other values shown that account for the cross-correlation of r_d with magnitude. The close agreement of this very different (and principally laboratory data based) approach, and the careful (field data based) probabilistic assessments of these current studies, are strongly mutually supportive.

Adjustments for Effective Overburden Stress:

An additional factor not directly resolved in prior studies based on field case histories is the increased susceptibility of soils to cyclic liquefaction, at the same CSR, with increases in effective overburden stress. This is <u>in addition</u> to the normalization of N-values for overburden effects as per Equation 4.

The additional effects of reduction of normalized liquefaction resistance with increased effective initial overburden stress (σ'_v) has been demonstrated by means of laboratory testing, and this is a manifestation of "critical state" type of behavior
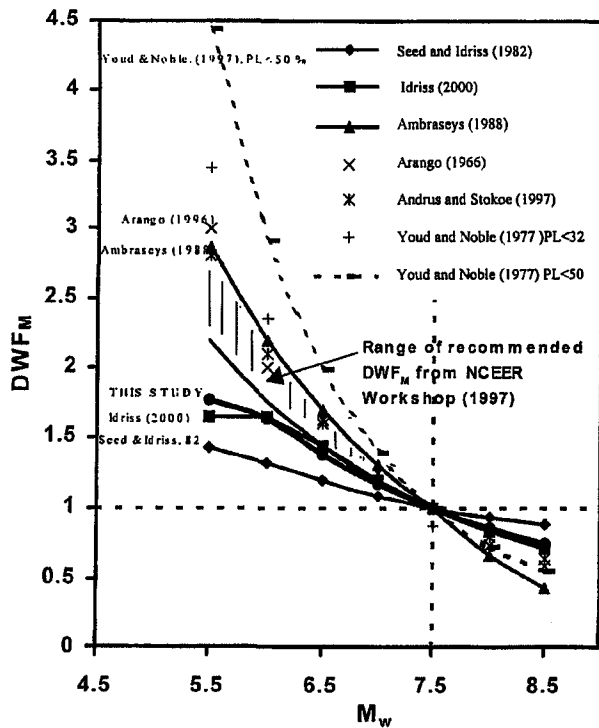
Fig.10(a): Previous Recommendations for Magnitude-Correlated Duration Weighting Factor, with Recommendations from Current Studies
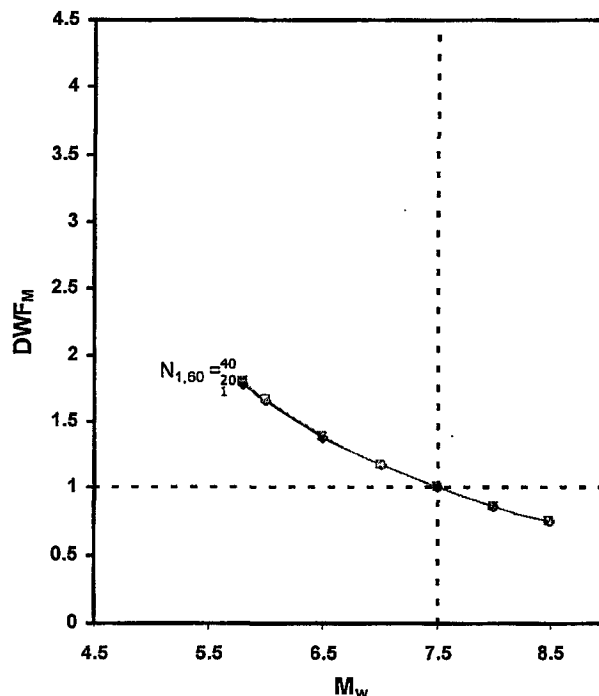

Fig. 10(b): Recommended Magnitude-Correlated Duration Weighting Factor as a Function of $N_{1,60}$

(soils become less dilatant at increased effective stress). Figure 13 shows the recommendations of the NCEER Working Group (Youd et al., 2001) regarding the correction factor K_σ to be used to correct to the normalized resistance to liquefaction at an initial effective overburden stress of 1 atm. ($CSR_{liq, 1atm}$) as

$$CSR_{liq} = CSR_{liq, 1atm} \cdot K_\sigma \qquad \text{(Eq. 9)}$$

These current studies were not very sensitive to K_σ, as the range of σ'_v in the case history data base was largely between $\sigma'_v = 600$ to $2,600$ lb/ft^2, but it was possible to "regress" K_σ as part of the Bayesian updating. The results are shown in Figure 14, over the range of $\sigma'_v \approx 600$ to $3,600$ lb/ft^2 for which they are considered valid. These are in good agreement with the earlier recommendations of Figure 13, and it is recommended that K_σ can be estimated as

$$K_\sigma = (\sigma'_v)^{f-1} \qquad \text{(Eq. 10)}$$

where $f \approx 0.6$ to 0.8 (as $N_{1,60,cs}$ varies from 1 to 40 blows/ft.) The field case history data of these current studies are <u>not</u> a sufficient basis for extrapolation of K_σ to much higher values of σ'_v, and the authors recommend use of Figure 13 for $\sigma'_v > 2$ atm.

The earlier relationships proposed by Seed et al. (1984), Liao et al. (1988, 1998), Youd and Noble (1997), and Toprak (1999) were all stated to be normalized to an effective overburden stress of approximately $\sigma'_v = 1$ atm (2,000 lb/ft^2). The correlation of Seed et al. (1984) was never formally corrected to $\sigma'_v = 1$ atm., however, as it was noted that the field case histories of the database were "shallow", and approximately in this range. The database was, however, <u>not</u> centered at $\sigma'_v = 1$ atm., but rather at lesser overburden (Mean $\sigma'_v \approx 1,300$ lb/ft^2 or 0.65 atm), and this proves to render this earlier relationship slightly unconservative if taken as normalized to $\sigma'_v = 1$ atm. (The same is true of all of the previous relationships discussed.) It should be noted, however, that this unconservatism is minimized if the correlations are applied at shallow depths.

For correctness, and to avoid ambiguity, both the earlier relationship of Seed et al. (1984), and the correlations developed in these current studies, need to be formally normalized to $\sigma'_v = 1$ atm. Accordingly, in these studies, <u>all</u> data are corrected for K_σ-effects (by Equations 9 and 10); not just those data for which σ'_v was greater than 1 atm. A recommended limit is $K_\sigma \leq 1.5$ (at very shallow depths.) Figures 12 and 13 show the proposed new correlations, this time for $\sigma'_v = 1$ atm, and these figures represent the <u>final</u>, fully normalized recommended correlations.

The overall correlation can be expressed in parts, as in the previous sections (and Equations 6 - 12, and Figures 7 - 12). It can also be expressed concisely as a single, composite relationship as shown in Equation 11.

$$P_L(N_{1,60}, CSR, M_w, \sigma_v', FC) = \Phi\left(-\frac{\begin{pmatrix} N_{1,60} \cdot (1 + 0.004 \cdot FC) - 13.32 \cdot \ln(CSR) - \\ 29.53 \cdot \ln(M_w) - 3.70 \cdot \ln(\sigma_v') \\ + 0.05 \cdot FC + 44.97 \end{pmatrix}}{2.70}\right) \quad \text{(Eq. 11)}$$

where

P_L = the probability of liquefaction in decimals (i.e. 0.3, 0.4, etc.)

Φ = the standard cumulative normal distribution. Also the cyclic resistance ratio, CRR, for a given probability of liquefaction can be expressed as:

$$CRR(N_{1,60}, CSR, M_w, \sigma_v', FC, P_L) = \exp\left[\frac{\begin{pmatrix} N_{1,60} \cdot (1 + 0.004 \cdot FC) - 29.53 \cdot \ln(M_w) \\ - 3.70 \cdot \ln(\sigma_v') + 0.05 \cdot FC + 44.97 + 2.70 \cdot \Phi^{-1}(P_L) \end{pmatrix}}{13.32}\right] \quad \text{(Eq. 12)}$$

where

$\Phi^{-1}(P_L)$ = the inverse of the standard cumulative normal distribution (i.e. mean=0, and standard deviation=1)

note: for spreadsheet purposes, the command in Microsoft Excel for this specific function is "NORMINV(P_L,0,1)"
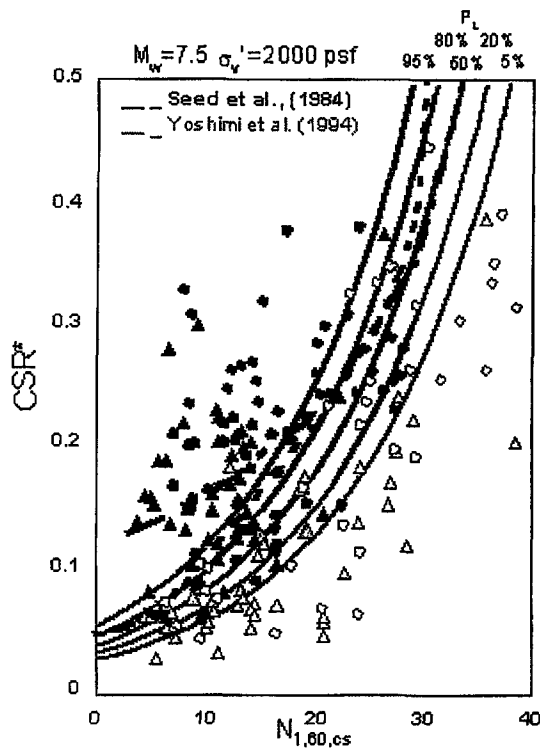

Fig. 11: Recommended "Deterministic" SPT-Based Liquefaction Triggering Correlation (for M_w=7.5 and σ_v'=1.0 atm) and the Relationship for "clean sands" Proposed by Seed et al. (1984)
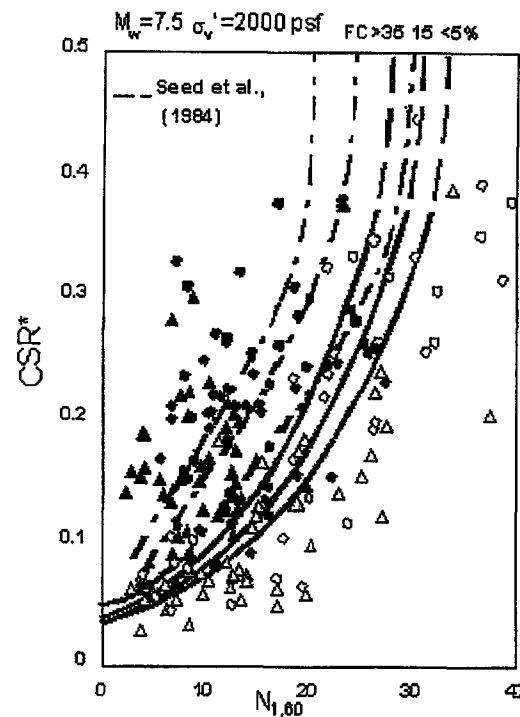
Fig. 12: Recommended "Deterministic" SPT-Based Liquefaction Triggering Correlation (for M_w=7.5 and σ_v'=1.0 atm) with Adjustments for Fines Content Shown.
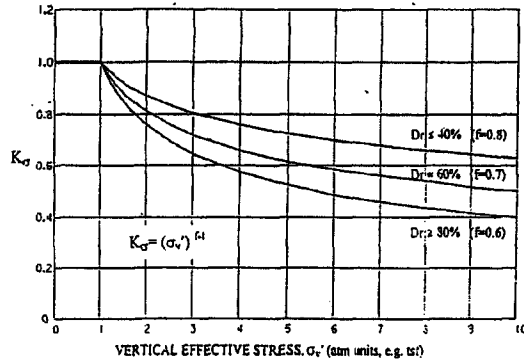
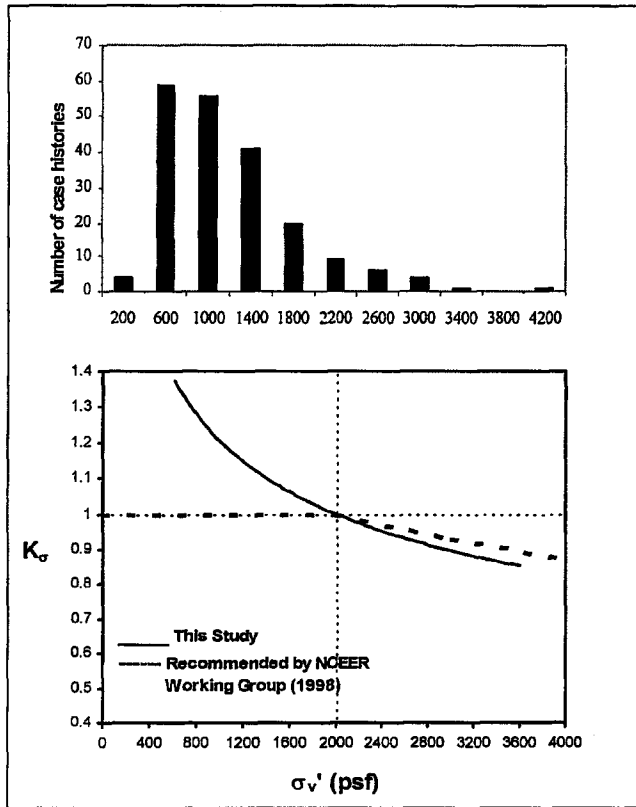**Fig. 13: Recommended K_σ Values for $\sigma'_v > 2$ atm.**

Fig. 14: Values of K_σ Developed and Used in These Studies, NCEER Working Group Recommendations (for n=0.7, $D_R \approx 60\%$) for Comparison

Recommended Use of the New SPT-Based Correlations:

The proposed new probabilistic correlations can be used in either of two ways. They can be used directly, all at once, as summarized in Equations 11 and 12. Alternatively, they can

be used "in parts" as has been conventional for most previous, similar methods. To do this, measured N-values must be corrected to $N_{1,60}$-values, using Equations 3, 4 and 5. The resulting $N_{1,60}$-values must then be further corrected for fines content to $N_{1,60,cs}$-values, using Equations 6 and 7 (or Figure 12). Similarly, in situ equivalent uniform cyclic stress ratio (CSR_{eq}) must be evaluated, and this must then be adjusted by the magnitude-correlated Duration Weighting Factor (DWF_M) using Equation 8 (and Figure 10) as

$$CSR_{eq,M=7.5} = CSR_{eq} / DWF_M \qquad \text{(Eq. 13)}$$

The new $CSR_{eq,M=7.5}$ must then be further adjusted for effective overburden stress by the inverse of Equation 9, as

$$CSR^* = CSR_{eq,M=7.5,1atm} = CSR_{eq,M=7.5} / K_\sigma \qquad \text{(Eq 14)}$$

The resulting, fully adjusted and normalized values of $N_{1,60,cs}$ and $CSR_{eq,M=7.5,1atm}$ can then be used, with Figure 11 to assess probability of initiation of liquefaction.

For "deterministic" evaluation of liquefaction resistance, largely compatible with the intent of the earlier relationship proposed by Seed et al. (1984), the same steps can be undertaken (except for the fines adjustment) to asses the fully adjusted and normalized $CSR_{eq,M=7.5,1atm}$ values, and normalized $N_{1,60}$ values, and these can then be used in conjunction with the recommended "deterministic" relationship presented in Figure 14. The recommendations of Figure 14 correspond to the new probabilistic relationships (for $P_L = 20\%$), except at very high CSR (CSR > 0.4). At these very high CSR; (a) there is virtually no conclusive field data, and (b) the very dense soils ($N_{1,60} \geq 30$ blows/ft) of the boundary region are strongly dilatant and have only very limited post-liquefaction strain potential. Behavior in this region is thus not conducive to large liquefaction-related displacements, and the heavy dashed lines shown in the upper portion of Figure 12 represent the authors' recommendations in this region based on data available at this time.

This section of this paper has presented the development of recommended new probabilistic and "deterministic" relationships for assessment of likelihood of initiation of liquefaction. Stochastic models for assessment of seismic soil liquefaction initiation risk have been developed within a Bayesian framework. In the course of developing the proposed stochastic models, the relevant uncertainties including: (a) measurement/estimation errors, (b) model imperfection, (c) statistical uncertainty, and (d) those arising from inherent variables were addressed.

The resulting models provide a significantly improved basis for engineering assessment of the likelihood of liquefaction initiation, relative to previously available models, as shown in Figure 5(d). The new models presented and described in this paper deal explicitly with the issues of (1) fines content (FC), (2) magnitude-correlated duration weighting factors (DWF_M),

and (3) effective overburden stress (K_σ effects), and they provide both (1) an unbiased basis for evaluation of liquefaction initiation hazard, and (2) significantly reduced overall model uncertainty. Indeed, model uncertainty is now reduced sufficiently that overall uncertainty in application of these new correlations to field problems is now driven strongly by the difficulties/uncertainties associated with project-specific engineering assessment of the necessary "loading" and "resistance" variables, rather than uncertainty associated with the correlations themselves. This, in turn, allows/encourages the devotion of attention and resources to improved evaluation of these project-specific parameters. As illustrated in Figures 5(d), 11 and 12, this represents a significant overall improvement in our ability to accurately and reliably assess liquefaction hazard.

CPT-, V_S- and BPT-Based Correlations:

In addition to SPT, three other in-situ index tests are now sufficiently advanced as to represent suitable bases for correlation with soil liquefaction triggering potential, and these are (a) the cone penetration test (CPT), (b) in-situ shear wave velocity measurement (V_S), and (c) the Becker Penetration Test (BPT).

The SPT-based correlations are currently better defined, and provide lesser levels of uncertainty, than these other three methods. CPT, however, is approaching near parity and can be expected to achieve a nearly co-equal status with regard to accuracy and reliability in the next few years.

CPT-based correlations have, to date, been based on much less numerous and less well defined earthquake field case histories than SPT-based correlations. This will change over the next few years, however, as at least five different teams of investigators in the U.S., Canada, Japan, and Taiwan are currently working (independently of each other) on development of improved CPT-based triggering correlations. This includes the authors of this paper, and it is our plan to have preliminary correlations available by the Fall of 2002. Approximately 650 earthquake field case histories (with CPT data) are currently available for possible use in development of such correlations, representing a tremendous increase over the number of cases available to the developers of currently available correlations. This increase is due mainly to large databases available from the recent 1994 Northridge, 1995 Kobe, 2000 Kocaeli (Turkey) and 2000 Chi-Chi (Taiwan) Earthquakes.

It is important to develop high quality CPT-based correlations to complement and augment the new SPT-based correlations presented herein. The authors are often asked whether SPT or CPT is intrinsically a better test for liquefaction potential evaluation. The correct answer is that both tests are far better when used together, as each offers significant advantages not available with the other.

SPT-based correlations are currently ahead of CPT-based correlations, due in large part to enhanced data bases and better data processing and correlation development. The new SPT-based correlations described in this paper are currently more accurate and reliable, and provide much lower levels of uncertainty or variance. An additional very significant advantage of SPT is that a sample is retrieved with each test, and so can be examined and evaluated to ascertain with certainty the character (gradation, fines content, PI, etc.) of the soils tested, as contrasted with CPT where soil character must be "inferred" based on cone tip and sleeve friction resistance data.

CPT offers advantages with regard to cost and efficiency (as no borehole is required). A second advantage is consistency, as variability between equipment and operators is small (in contrast to SPT). The most important advantage of CPT, however, is continuity of data over depth. SPT can only be performed in 18-inch increments, and it is necessary to advance and clean out the borehole between tests. Accordingly, SPT can only be performed at vertical spacings of about 30 inches (75cm) or more. As a result, SPT can completely miss thin (but potentially important) liquefiable strata between test depths. Similarly, with a 12-inch test height and allowance for effects of softer overlying and underlying strata, SPT can fail to suitably characterize strata less than about 3 to 4 feet in thickness.

CPT, in contrast, is fully continuous and so "misses" nothing. The need to penetrate about 4 to 5 diameters into a stratum to develop full tip resistance, to be at least 4 to 5 diameters from an underlying softer stratum, and the "drag length" of the following sleeve, cause the CPT test to poorly characterize strata of less than about 12 to 15 inches (30 to 40cm) in thickness, but this allows for good characterization of much thinner strata than SPT. Even for strata too thin to be adequately (quantifiably) characterized, the CPT at least provides some indications of potentially problematic materials if one examines the q_c and f_s traces carefully.

With the new SPT-based correlations available as a basis for cross-comparison, it is now possible to better assess currently available CPT-based correlations. Owing to its attractive form and simplicity, the CPT-based correlation of Robertson and Wride (1998) is increasingly used for liquefaction studies. This correlation is described in the NCEER summary papers (NCEER, 1997; Youd, et al., 2001). Preliminary cross-comparison with the new SPT-based correlation presented in this paper suggests that this CPT-based correlation is somewhat unconservative for relatively "clean" sandy soils (soils with less than about 5 to 10% fines), and is increasingly unconservative as fines content (and fines plasticity) increase. Robertson and Wride had access to a much smaller field case history database than is currently available, and so their correlation represents a valuable interim contribution as we continue to await development of new correlations in progress in several quarters (as discussed previously.) Until the new CPT-based correlations become available, the correlation of Robertson and Wride can be modified slightly to provide improved apparent agreement with the new SPT-based correlation.
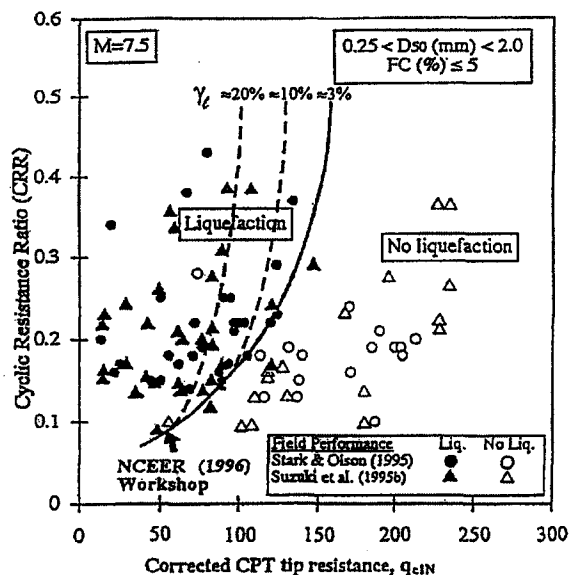
Fig. 15: CPT-Based Liquefaction Triggering Correlation for "Clean" Sands Proposed by Robertson and Wride (1998)
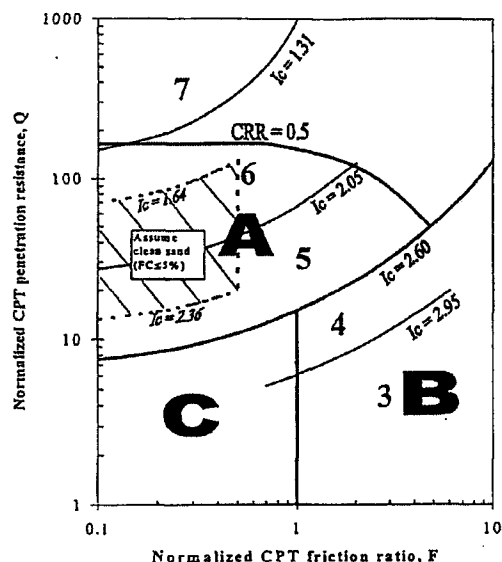

Zone A: Cyclic liquefaction possible – depends on size and duration of cyclic loading.
Zone B: Liquefaction unlikely – check other criteria.
Zone C: Flow/cyclic liquefaction possible – depends on soil plasticity and sensitivity as well as size and duration of cyclic loading.

Fig. 16: Limitations in Fines Correction as Proposed by Robertson and Wride(1998)

Figure 15 shows the "baseline" triggering curve of Robertson and Wride for "clean" sandy soils. Adjustments for fines are based on combinations of sleeve friction ratios and tip resistances in such a manner that the "clean sand" boundary curve of Figure 15 is adjusted based on a composite parameter

I_C. I_C is a measure of the distance from a point above and to the left of the plot of normalized tip resistance ($q_{c,1}$) and normalized Friction Ratio (F) as indicated in Figure 16. The recommended "fines" correction is a nonlinear function of I_C, and ranges from 1.0 at $I_C = 1.64$ to a maximum value of 3.5 at $I_C = 2.60$. A further recommendation on the fines correction factor is that this factor be set at 1.0 in the shaded zone within Area "A" of Figure 16 (within which $1.64 < I_C < 2.36$ and F < 0.5).

Based on cross-comparison with the new SPT-based correlation, it appears that improved compatibility can be accomplished by shifting the baseline triggering curve for "clean" sands of Figure 15 to the right by about 25 kg/cm², and by further limiting the maximum fines adjustment factor to not more than about 2. An additional area of concern occurs at the base of the shaded zone within Area "A" of Figure 16, as the recommendations of Robertson and Wride lead to a "jump" in the fines correction factor at this location, and the soils in this region (with very low tip resistances, $q_{c,1}$) can be very dangerous materials. It is suggested that the shaded zone within area "A" of Figure 16 be extended, and that the "fines correction" be taken as 1.0 for F<0.5 at all $q_{c,1}$ values. These adjustments are interim measures only, and the resulting "adjusted" correlation is not intended to provide either the accuracy or the reliability available with the new SPT-based correlation, but rather an improved interim level of compatibility and conservatism as researchers work to develop updated correlations.

V_S-based correlations are very attractive because V_S can be measured with non-intrusive methods (e.g. Spectral Analysis of Surface Waves (SASW)) and can provide both a potentially rapid screening method, and a method for assessment of coarse, gravelly soils which cannot be reliably penetrated or reliably characterized with small diameter penetrometers (SPT and CPT).

At this time, the best V_S-based correlation available is that of Andrus and Stokoe (2000). This V_S-based correlation is also described in the NCEER Workshop summary papers (NCEER, 1997; Youd et al., 2001.) Although it is certainly the best of its type, this correlation is less well-defined (more approximate) than either SPT- or CPT-based correlations. This is not due only to lack of data (though the V_S field case history database is considerably smaller than that available for SPT and CPT correlation development). V_S does not correlate as reliably with liquefaction resistance as does penetration resistance because V_S is a very small-strain measurement and correlates poorly with a very "large-strain" phenomenon (liquefaction). Small amounts of "aging" and cementation of interparticle contacts can cause V_S to increase more rapidly than the corollary increase in liquefaction resistance. V_S-based correlations for resistance to "triggering" of liquefaction are thus best employed either conservatively, or as preliminary screening tools to be supplemented by other methods.

Coarse, gravelly soils can be especially problematic with regard to evaluation of resistance to "triggering" of

liquefaction, as large particles (gravel-sized and larger) can impede the penetration of both SPT and CPT penetrometers. As large-scale frozen sampling and testing are too expensive for conventional projects, engineers faced with the problem of coarse, gravelly soils generally have three options available here.

One option is to employ V_S-based correlations. V_S measurements can be made in coarse soils, either with surface methods (e.g. SASW, etc.) or via borings. V_S-based correlations are somewhat approximate, however, and so should be considered to provide conclusive results only for deposits/strata that are clearly "safe" or clearly likely to liquefy.

A second option is to attempt "short-interval" SPT testing. This can be effective when the non-gravel (finer than about 0.25 inch diameter) fraction of the soil represents greater than about half of the overall soil mix/gradation. (Note that it is approximately the D_{30} and finer size range that controls the liquefaction behavior of such soils.) Short-interval SPT involves performing the SPT in the standard manner, but counting the blow count (penetration resistance) in 1-inch increments rather than 6-inch increments. (When penetration is more than 1-inch for a single blow, a fractional blow count of less than 1 blow/inch is credited.) The resulting history of blows/inch is then plotted for each successive inch (of the 12-inches of the test). When values (per inch) transition from low to high, it is assumed that a coarse particle was encountered and impeded the penetrometer. High values are discarded, and the low values are summed, and then scaled to represent the equivalent number of blows per 12-inches. (e.g.: If it is judged that 7 of the inches of penetration can be "counted", but that 5 of the inches must be discarded as unrepresentatively high, then the sum of the blows per the 7 inches is multiplied by 12/7 to derive the estimated overall blow count as blows/12 inches.)

This approach has been shown to correlate well with BPT values from the larger-scale Becker Penetrometer for soils with gravel-plus sized fractions of less than about 40 to 50%. It is noted, however, that the corrected short-interval SPT blow counts can still be biased to the high side due to unnoticed/undetected influence of coarse particles on some of the penetration increments used, so that it is appropriate to use lower than typical enveloping of the resulting blow counts to develop estimates of "representative" N-values for a given stratum (e.g.: 20 to 30-percentile values, rather than 35 to 50-percentile values as might have been used with regular SPT in soils without significant coarse particles).

When neither V_S-based correlations nor short-interval SPT can sufficiently characterize the liquefaction resistance of coarse soils, the third method available is the use of the large-scale Becker Penetrometer. Essentially a large-diameter steel pipe driven by a diesel pile hammer (while retrieving cuttings pneumatically), the Becker Penetrometer (BPT) resistance can be correlated with SPT to develop "equivalent" N-values (N_{BPT}). Care is required in monitoring the performance of the

BPT, as corrections must be made for driving hammer bounce chamber pressures, etc. (see Harder, 1997). The best current BPT correlation (with SPT) for purposes of liquefaction engineering applications is described by Harder (1997), NCEER (1997), and Youd et al. (2001). BPT has been performed successfully for liquefaction evaluations in soils with maximum particles sizes (D_{100}) of up to 1 m. and more, and to depths of up to 70 m. The BPT is a large and very noisy piece of equipment, however, and both cost and site access issues can be problematic.

ASSESSMENT OF POST-LIQUEFACTION STABILITY

Once it has been determined that initiation or "triggering" of liquefaction is likely to occur, the next step in most liquefaction studies is to assess "post-liquefaction" global stability. This entails evaluation of post-liquefaction strengths available, and comparison between these strengths and the driving shear stresses imposed by (simple, non-seismic) gravity loading. Both overall site stability, and stability of structures/facilities in bearing capacity, must be evaluated. If post-liquefaction stability under simple gravity loading is not assured, then "large" displacements and/or site deformations can ensue, as geometric rearrangement is necessary to re-establish stability (equilibrium) under static conditions.

The key issue here is the evaluation of post-liquefaction strengths. There has been considerable research on this issue over the past two decades (e.g.: Jong and Seed, 1988; Riemer, 1992; Ishihara, 1993; etc.). Two general types of approaches are available for this. The first is use of sampling and laboratory testing, and the second is correlation of post-liquefaction strength behavior from field case histories with in-situ index tests.

Laboratory testing has been invaluable in shedding light on key aspects of post-liquefaction strength behavior. The available laboratory methods have also, however, been shown to provide a generally unconservative basis for assessment of in-situ post-liquefaction strengths. The "steady-state" method proposed by Poulos, Castro and France (1986), which used both reconstituted samples as well as high-quality "slightly" disturbed samples, and which provided a systematic basis for correction of post-liquefaction "steady-state" strengths for inevitable disturbance and densification that occurred during sampling and re-consolidation prior to undrained shearing, provided an invaluable incentive for researchers. The method was eventually found to produce post-liquefaction strengths that were much higher than those back-calculated from field failure case histories (e.g.: Von Thun, 1986; Seed et al., 1989).

Reasons for this included: (1) the very large corrections required to account for sampling and reconsolidation densification prior to undrained shearing, (2) sensitivity to the assumption that the steady-state line (defining the relationship between post-liquefaction strength, $S_{u,r}$ vs. void ratio, e) which was evaluated based on testing of fully remolded (reconstituted) samples provides a basis for "parallel"

correction for this unavoidable sample densification, (3) use of C-U triaxial tests, rather than simple shear tests, for field situations largely dominated by simple shear, (4) reconsolidation of samples to higher than in-situ initial effective stresses, and (5) the failure of laboratory testing of finite samples to account for the potentially important effects of void redistribution during "undrained" shearing in the field.

It has now been well-established that both simple shear and triaxial extension testing provide much lower undrained residual strengths than does triaxial compression (e.g.: Riemer, 1992; Vaid, 1990; Ishihara, 1993; etc.), often by factors of 2 to 5, and simple shear tends to be the predominant mode of deformation of concern for most field cases. Similarly, it is well-established that samples consolidated to higher initial effective stresses exhibit higher "residual" undrained strengths at moderate strains (strains of on the order of 15 to 30%), and this range of strains represents the limit of accurate measurements for most testing systems.

These issues can be handled by performing laboratory tests at field in-situ initial effective stress levels, and by performing undrained tests in either simple shear or torsional shear. The remaining unresolved issues that continue to preclude the reliable use of laboratory testing as a basis for assessment of in-situ (field) post-liquefaction strengths are two-fold. The first of these is the difficulty in establishing a fully reliable basis for correction of laboratory test values of $S_{u,r}$ for inevitable densification during both sampling and laboratory reconsolidation prior to undrained shearing. The correction factors required, for loose to medium dense samples, are routinely on the order of 3 to 20, and there is no proven reliable basis for these very large corrections. Use of frozen samples does not fully mitigate this problem, as volumetric densification due to reconsolidation upon thawing (prior to undrained shearing) continues to require large corrections here.

The second problem is intrinsic to the use of any laboratory testing of finite samples for the purpose of assessment of in-situ (field) post-liquefaction strengths, and that is the very important issue of void redistribution. Field deposits of soils of liquefiable type, both natural deposits and fills, are inevitably sub-stratified based on local variability of permeability. This produces "layers" of higher and lower permeability, and this layering is present in even the most apparently homogenous deposits. During the "globally undrained" cyclic shearing that occurs (rapidly) during an earthquake, a finite sublayer "encapsulated" by an overlying layer of at least slightly lower permeability can be largely isolated and may perform in a virtually undrained manner, remaining essentially at constant volume. Although the sublayer loses no volume, however, there is a progressive rearrangement of the solids and pore fluid within the sublayer as the soils cyclically soften and/or liquefy. This progressive rearrangement, which causes the solid particles to settle slightly and thus increase the density in the lower portion of the sub-layer, while simultaneously reducing the density of the

top of the sublayer, is "localized void redistribution" during globally undrained shearing.

Owing to the very sensitive relationship between post-liquefaction strength ($S_{u,r}$) and void ratio (e) for loose to medium density soils, even apparently minor amounts of increase in void space (reduction in dry density) at the top of a sub-layer can result in large reductions in $S_{u,r}$. In extreme cases, water attempting to escape from the sublayer can be temporarily trapped by the overlying, less pervious layer, and can form a "film" or water-filled "blister" at the interface between the two layers (in which case the shear strength, $S_{u,r}$, is reduced fully to zero along this interface.)
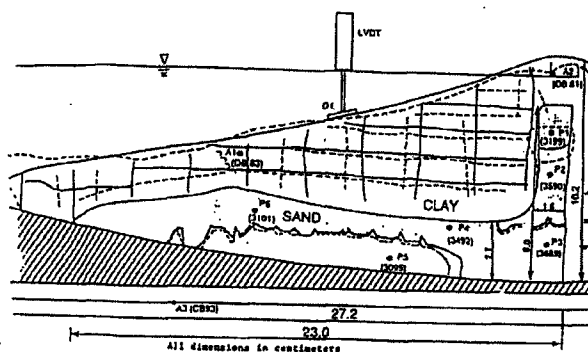

Fig. 17: Post-Failure Configuration of Centrifuge Test Slope (after Arulanandan et al., 1993)

An interesting early example of this behavior was produced in a centrifuge test performed by Arulanandan et al. (1993), as illustrated in Figure 17. In this experiment, an embankment was constructed with a sand "core" and a surrounding clay "shell" to prevent drainage during cyclic loading. The sand core was marked with layers of black sand so that localized changes in volume (and density) could be tracked during globally undrained shearing. When subjected to a model earthquake, cyclic pore pressure generation within the sand occurred, and the embankment suffered a stability failure. During the "undrained" earthquake loading, the overall volume of the saturated sand "core" remained constant, satisfying the definition of globally undrained loading. Locally, however, the lower portions of the sand "core" became denser, and the upper portions suffered corollary loosening. The top of the sand layer suffered the greatest loosening, and it was along the top of this zone of significantly reduced strength that the slope failure occurred.

Given the propensity for occurrence of localized void redistribution during seismic loading, and the ability of Nature to selectively push failure surfaces preferentially through the resulting weakened zones at the tops of localized sub-strata (and water blisters in worst-cases), the overall post-liquefaction strength available is a complex function of not only initial (pre-earthquake) soil conditions (e.g. density, etc.), but also the scale of localized sub-layering, and the relative orientations and permeabilities of sub-strata. These are not qualities that can be reliably characterized, at this time, by
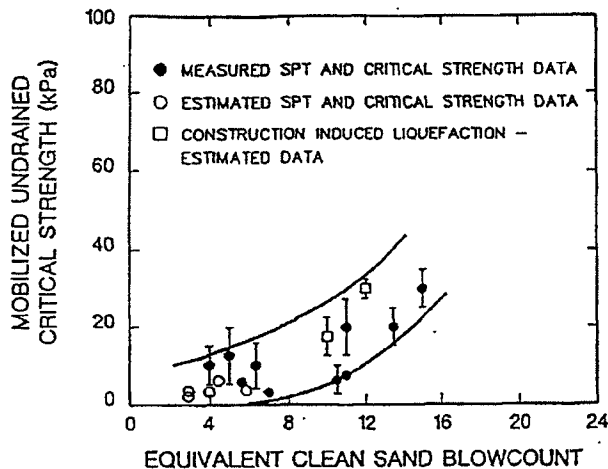
Fig. 18: Recommended Relationship Between $S_{u,r}$ and $N_{1,60,CS}$ (Seed and Harder, 1990)
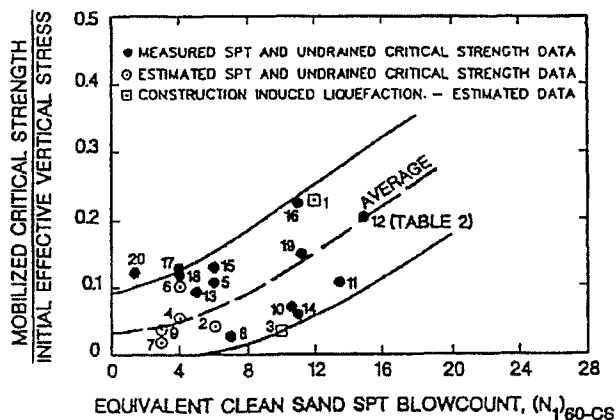

Fig. 19: Relationship Between $S_{u,r}/P$ vs. $N_{1,60,CS}$ as Proposed by Stark and Mesri (1992)

laboratory testing of soil samples (or "elements") of finite dimensions.

Accordingly, at this time, the best basis for evaluation of post-liquefaction strengths is by development of correlations between in-situ index tests vs. post-liquefaction strengths back-calculated from field case histories. These failure case histories necessarily embody the global issues of localized void redistribution, and so provide the best indication available at this time regarding post-liquefaction strength for engineering projects.

Figure 18 presents a plot of post-liquefaction residual strength ($S_{u,r}$) vs. equivalent clean sand SPT blow count ($N_{1,60,cs}$). This was developed by careful back analyses of a suite of liquefaction failures, and it should be noted that these types of back analyses require considerable judgement as they are sensitive to assumptions required for treatment of momentum and inertia effects. The difficulties in dealing with these momentum/inertia effects (which are not an issue in

conventional "static" stability analyses) are an important distinction between the efforts of various investigators to perform back-analyses of these types of failures. In this figure, the original correction for fines used to develop $N_{1,60,cs}$ is sufficiently close to that of Equations 6 and 7, that Equations 6 and 7 can be used for this purpose.

Stark and Mesri (1992), noting the influence of initial effective stress on $S_{u,r}$, proposed an alternate formulation and proposed a correlation between the ratio of $S_{u,r}/P$ and $N_{1,60,cs}$, as shown in Figure 19, where P is the initial major principal effective stress ($\sigma'_{1,i}$). This proposed relationship overstates the dependence of $S_{u,r}$ on $\sigma'_{1,i}$, and so is overconservative at shallow depths ($\sigma'_{1,i} < 1$ atmosphere) and is somewhat unconservative at very high initial effective stresses ($\sigma'_{1,i} > 3$ atmospheres).

It is also true, however, that the relationship of Figure 18 understates the influence of $\sigma'_{1,i}$ on $S_{u,r}$. Figure 20 shows an excellent example of this. Figure 20(a) shows the stress paths for a suite of four IC-U triaxial tests performed on samples of Monterey #30 sand, all at precisely the same density, but initially consolidated to different effective stresses prior to undrained shearing. (The sample void ratios shown are post-consolidation void ratios.) As shown in this figure, the samples initially consolidated to higher effective stresses exhibited higher undrained residual strengths ($S_{u,r}$). The ratio between $S_{u,r}$ and P was far from constant, however, as shown in Figure 20(b).

The influence of $\sigma'_{1,i}$ on $S_{u,r}$ (and on the ratio of $S_{u,r}/P$) is a function of both density and soil character. Very loose soils, and soils with higher fines contents, exhibit $S_{u,r}$ behavior that is more significantly influenced by $\sigma'_{1,i}$ than soils at higher densities and/or with lower fines content. At this time, the authors recommend that the relationship of Figure 18 (Seed & Harder, 1990) be used as the principal basis for evaluation of in-situ $S_{u,r}$ for "relatively clean" sandy soils (Fines Content < 12%). For these soils it is recommended that both relationships of Figures 18 and 19 be used, but that a 4:1 weighting be employed in favor of the values from Figure 18. Similarly, a more nearly intermediate basis (averaging the results of each method, with 2:1 weighting between the relationships of Figures 18 and 19) is recommended for very silty soils (Fines Content > 30%). For fines contents between 12% and 30%, a linear transition in weighting between the two proposed relationships can be used.

It must be noted that engineering judgement is still required in selection of appropriate post-liquefaction strengths for specific project cases. Consideration of layering and sub-layering, permeability/drainage, and potential void redistribution, and the potential for confluence of alignment of layering interfaces with shear surfaces must all be considered. For most "typical" cases, use of $S_{u,r}$ values in the lower halves of the ranges shown in Figures 18 and 19 (with due consideration for weighting of these) appears to represent a suitably prudent range for most engineering purposes at this time, but lower overall average post-liquefaction strengths can be realized
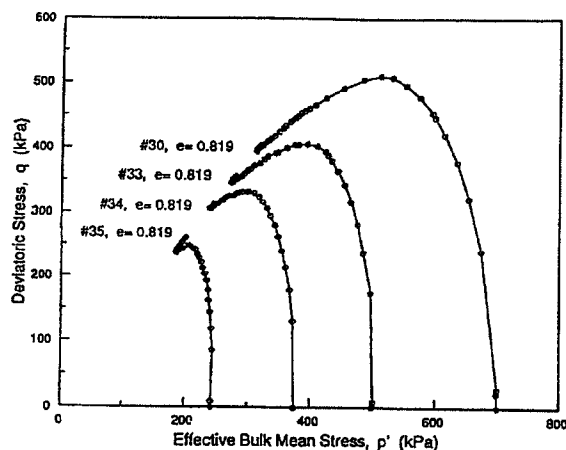
(a) Stress Paths
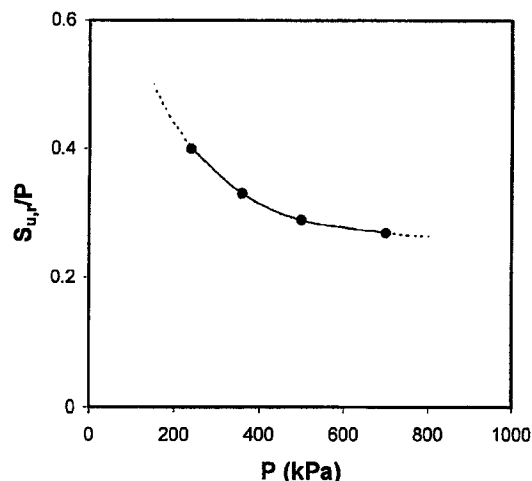
(b) Ratio of $S_{u,r}/P$ vs. P

Fig. 20: Results of IC-U Triaxial Tests on Monterey #30/0 Sand (After Riemer, 1992)

when layering and void redistribution combine unusually adversely with potentially critical failure modes.

Finally, a common question is "what happens at $N_{1,60,cs}$ values greater than about 15 blows/ft.?" The answer is that the relationships of Figures 18 and 19 should be concave upwards (to the right), so that extrapolation at constant slope to the right of $N_{1,60,cs}$=15 blows/ft should provide a conservative basis for assessment of $S_{u,r}$ in this range. As these projected values represent relatively good strength behavior, this linear extrapolation tends to be sufficient for most projects. It should be noted, however, that values of $S_{u,r}$ should generally not be taken as higher than the maximum <u>drained</u> shear strength. Values of $S_{u,r}$ higher than the fully-drained shear strength

would suggest significant dilation. Dilation of this sort tends to rapidly localize the shear zone (or shear band), and so reduces the drain path length across which water must be drawn to satisfy the dilational "suction". As these distances can be small, rapid satisfaction of this dilational demand is possible, and "undrained" (dilational) shear strengths higher than the drained strength can persist only briefly. Accordingly, for most engineering analyses the use of the fully drained shear strength as a maximum or limiting value is prudent. Similarly, the maximum shear strength cannot exceed the shear strength which would be mobilized at the effective stress corresponding to "cavitation" of the pore water (as it reaches a pore pressure of −1 atmosphere). The above limit to not more than the fully-drained strength is a stronger or more limiting constraint, however, and so handles this problem as well.

EVALUATION OF ANTICIPATED LIQUEFACTION-INDUCED DEFORMATIONS AND DISPLACEMENTS

Engineering assessment of the deformations and displacements likely to occur as a result of liquefaction or pore-pressure-induced ground softening is a difficult and very challenging step in most projects, and this is an area where further advances are needed.

Assessment of "Large" Liquefaction-Induced Displacements:

For situations in which the post-liquefaction strengths are judged to be less than the "static" driving shear stresses, deformations and displacements can be expected to be "large"; generally greater than about 1m., and sometimes much greater. Figure 21 shows examples of global site instability corresponding to situations wherein post-liquefaction strengths are less than gravity-induced driving shear stresses. These are schematic illustrations only, and are not to scale.

For most engineering projects, the "large" deformations associated with post-liquefaction "static instability" are unacceptably large, and engineering mitigation is thus warranted. It is often, therefore, not necessary to attempt to make quantified estimates of the magnitudes of these "large" deformations. Exceptions can include dams and embankments, which are sometimes engineered to safely withstand liquefaction-induced displacements of more than 1m.

Estimates of the "large" deformations likely to occur for these types of cases can often be made with fair accuracy (within a factor of about ± 2). "Large" liquefaction-induced displacements/deformations (> 1m.) are principally the result of gravity-induced "slumping", as geometric rearrangement of the driving soil and/or structural masses is required to re-establish static equilibrium. A majority of the deformations, for these cases, occur after strong shaking has ceased so that cyclic inertial forces are not very important in "driving" the deformations (though they <u>are</u> very important in "triggering" the liquefaction-induced ground softening.)

⊞ - Liquefied zone with low residual undrained strength

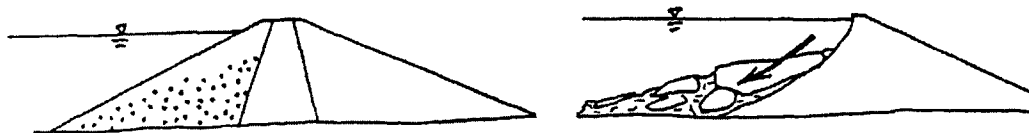(a) Edge Failure/Lateral Spreading by Flow
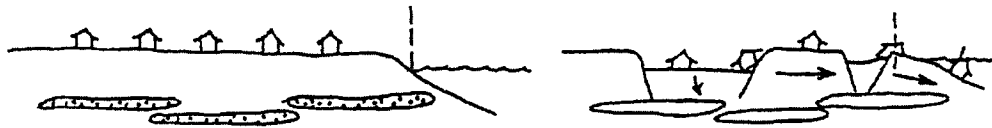
(b) Edge Failure/Lateral Spreading by Translation

(c) Flow Failure

(d) Translational Displacement

(e) Rotational and/or Translational Sliding

Fig. 21: Schematic Examples of Liquefaction-Induced Global Site Instability and/or "Large" Displacement Lateral Spreading

Three general types of approaches can be used to estimate expected "large" liquefaction-induced ground deformations, and these are: (1) fully nonlinear, time-domain finite element or finite difference analyses (e.g.: Finn et al., 1986; Byrne et al., 1998; France et al., 2000; etc.), (2) statistically-derived empirical methods based on back-analyses of field earthquake case histories (e.g.: Hamada et al, 1987; Bartlett and Youd, 1995; etc.), and (3) simple static limit equilibrium analyses coupled with engineering judgement. When applied with good engineering judgement, and when the critical deformation/displacement modes are correctly identified and suitable post-liquefaction strengths are selected, all three methods can provide reasonable estimates of the magnitudes of expected displacements.

Finite element and finite difference analyses are the most complex of the three approaches, and we cannot reasonably discuss these in detail within the confines of this paper. These methods have, to date, principally been employed mainly for relatively critical (and well-budgeted) studies, but growing comfort with these methods (coupled with decreasing computing costs) can be expected to bring these types of analyses more into the mainstream. The principal difficulty associated with these methods is the difficulty of evaluating the model "input" parameters necessary for the relatively complex behavioral and/or constitutive models used. These models are usually "sensitive" to relatively minor variations in one or more parameters, and assessment of this type of parameter sensitivity is a vital element of such studies.

The second type of methods available are the "Hamada-type" empirical methods for estimation of lateral displacements due to liquefaction-induced lateral spreading. These methods are based on back-analyses of lateral spreading case histories, and involve probabilistically and/or statistically derived empirical equations for estimation of expected lateral spreading displacements. Currently, the most widely used such method in the western U.S. is that of Bartlett and Youd, 1995. This method addresses two types of cases: cases where there is a "free face" towards which lateral spreading can occur (e.g.: Figures 21(a) and 21(b)), and cases without a free face but with a sloping ground surface (e.g.: Figures 21(c) and 21 (d)). Two different empirical equations are provided, one for each of these two situations.

Figure 22 shows the results of this approach (both equations, as applicable.) Figure 22(a) shows a plot of predicted displacement magnitude vs. the actual observed displacement for the case histories studied. For (measured) displacements greater then approximately 1.5m., the ratio of predicted:measured displacements was generally in the range of 0.5:1 to 2:1, and this is a reasonable band of accuracy for engineering purposes in this range of displacements.

The third method for estimation of expected "large" liquefaction-induced displacements is based on evaluation of the deformations/displacements required to re-establish static equilibrium. This requires careful assessment of the most critical mode of failure/deformation. An important issue in
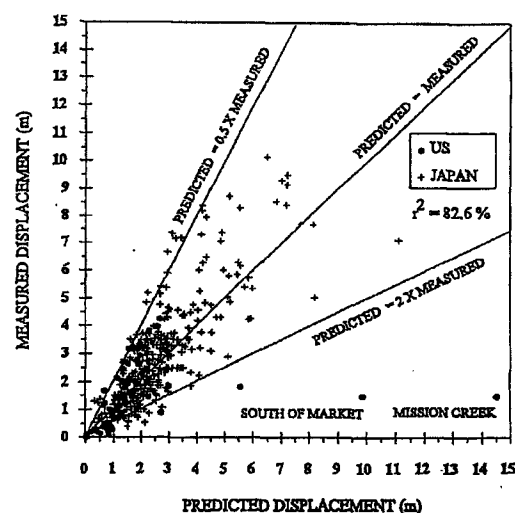
(a)   Measured vs. Predicted Displacements, All Case Histories
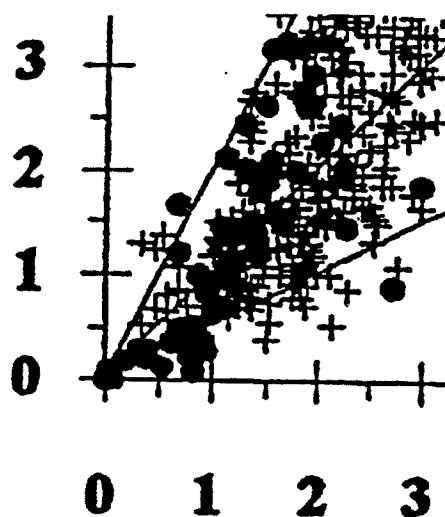
(b) Measured vs. Predicted Displacements for Cases with Maximum Displacements of Less Than 3m

Fig. 22: Predicted vs. Measured Displacements from Lateral Spreading Case Histories (after Bartlett and Youd, 1995)

this approach is the progressive acceleration and then deceleration of the displacing soil (and/or structural) mass. The deformations are not arrested when the geometry is sufficiently rearranged as to produce a "static" Factor of Safety of 1.0 (based on post-liquefaction strengths, as appropriate.). Instead, shear strength must be employed to overcome the momentum progressively accumulated during acceleration of the displacing mass, so that the deforming mass comes to rest at a "static" Factor of Safety of greater

than 1.0 (FS ≅ 1.05 to 1.25 is common, depending on the maximum velocity/momentum achieved before deceleration). For many problems, simply estimating the degree of geometry rearrangement necessary to produce this level of Factor of Safety (under "static" conditions, but with post-liquefaction strengths) can produce fair estimates of likely displacements. Alternatively, incremental calculations of (1) overall stability (excess driving shear stresses), (2) acceleration (and then deceleration) of the displacing mass due to shear stress imbalance (vs. shear strength), (3) accrual and dissipation of velocity (and momentum), and (4) associated geometry rearrangement, can produce reasonable estimates of likely ranges of displacements for many cases.

Finally, it should be noted that these three types of approaches for estimation of expected "large" liquefaction-induced displacements and deformations can be used to cross-check each other. For example, it is prudent to check the final geometry "predicted" by the results of finite element or finite difference analyses for its "static" Factor of Safety (with post-liquefaction strengths.)

Assessment of "Small to Moderate" Liquefaction-Induced Displacements:

Although it is feasible to make reasonably accurate estimates of post-liquefaction deformations and displacements for cases of "large" displacements, we currently do not have tools for accurate and reliable estimation of "small to moderate" liquefaction-induced displacements (displacements/deformations of less than about 0.75m.) Unfortunately, it is this "small to moderate" range of 0 to 0.75m. that is most important for most conventional buildings and engineered facilities.

Unlike the case of "large" liquefaction-induced displacements, which are dominated by displacements "driven" principally by gravity forces after the cessation of strong shaking, "small to moderate" displacements are very strongly affected by cyclic inertial forces produced by strong shaking. In addition, "small to moderate" displacements are usually controlled in large part by complicated cyclic, pore pressure-induced softening followed by dilation and corollary reduction in pore pressures (and consequent re-establishment of strength and stiffness.) This softening and re-stiffening behavior is relatively complex and difficult to predict with good accuracy and reliability.

Figures 23 through 25 illustrate the complicated types of mechanical behaviors that control cyclic deformations in this "small to moderate" displacement range. Figure 23 presents the results of an undrained cyclic simple shear test of Monterey #0/30 sand at a relative density of $D_r = 50\%$, and an initial vertical effective stress of $\sigma'_{v,i} = 85$ kPa. These conditions correspond roughly to a soil with an $N_{1,60,cs}$ value of about 10 blows/ft. In this figure, (a) the bottom left figure presents evolution of cyclically-induced pore pressures (expressed as reduction in $\sigma'_{v,i}$), (b) the bottom right figure shows increasing shear strains with increasing numbers of cycles, (c) the top right figure shows shear stress vs. shear

strain behavior, and (d) the top left figure presents the effective stress path followed during this test. All four sub-figures are scaled so that the axes of the figures to the side and/or above and below each share commonly scaled axes.

As shown in Figure 23, shear strains are relatively small for the first 25 cycles, until significant cyclically-induced pore pressures have been generated. At that point (after about 25 cycles), there is a rapid increase in cyclic shear strains, representing "triggering" of liquefaction. Examining the stress path plots (and also the stress-strain and cyclic pore pressure generation plots) shows clearly that pore pressures are generated upon initial reversal of cyclic shear stresses during each half-cycle of loading, but that dilation ensues later in each cycle as shear strains begin to increase in the new direction of loading. This process of cyclic softening and then re-stiffening during each cycle is now well understood, but remains difficult to model reliably for non-uniform (irregular) cyclic loading, as in earthquakes.

Figure 24 similarly shows the same suite of plots for an undrained cyclic simple shear test on a sample of the same sand, but this time at an initial relative density of $D_r = 75\%$. This corresponds roughly to an in situ $N_{1,60,cs}$ value of about 25 to 30 blows/ft. Denser soils in this range exhibit very different behavior than the looser sample of Figure 23.

The cyclic stress ratio of the test presented in Figure 24 is 1.8 times higher than that of the previous figure. The denser sample (Figure 24) is more strongly dilatant with each half-cycle of loading, and instead of relatively "suddenly" beginning a rapid rate of increase of shear strains (as in the previous test), this denser sample exhibits a more moderate (and less dramatically accelerating) rate of increase of cyclic shear strains. Indeed, as there is no sudden transition in behaviors, it is difficult to identify a singular point at which "triggering" of liquefaction can be said to occur. At this time, it is recommended that "triggering" or initiation of liquefaction be considered to have occurred when a soil has experienced significant cyclic pore pressure generation (and attendant softening and loss of strength), and has reached a cyclic shear strain (in either single direction) of $\gamma \cong 3\%$. At this level of shear strain, subsequent performance (including "post-liquefaction" strength and stress-deformation behavior) will be controlled largely by the soil's contractive or dilational behaviors.

Further complicating the issue of prediction of liquefaction-induced deformations is the fact that, for most cases of engineering interest, there is a directionally preferential "driving" shear stress due to gravity loading (in addition to cyclic inertial stresses induced by the earthquake). Figure 25 presents the results of an undrained cyclic simple shear test with these initial "driving" shear stresses. In this test, the "driving" shear stresses are aligned in the same direction as the (reversing) cyclic shear stress loading, and the initial (constant) driving shear stresses are equal to 0.08 times the initial vertical effective stress (of 85 kPa).
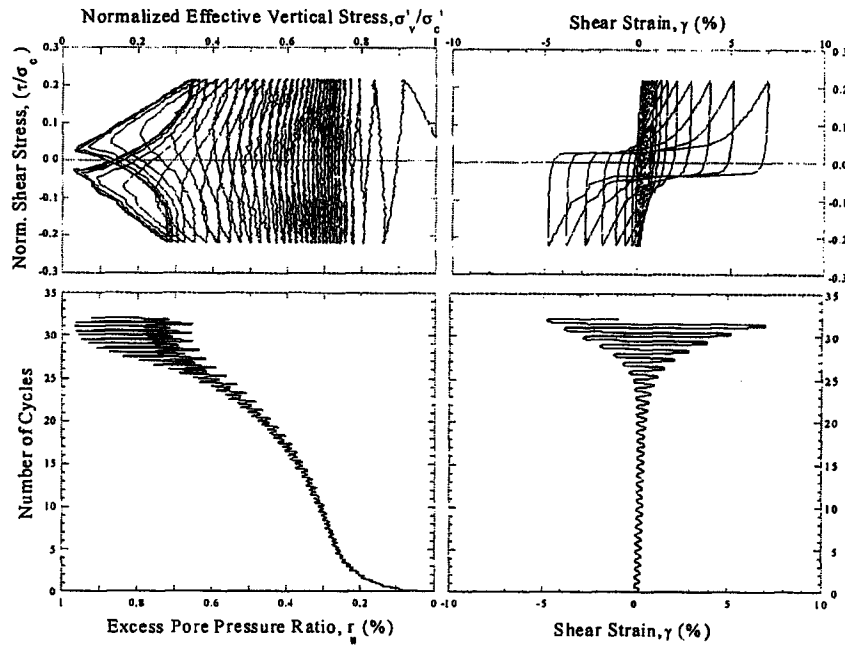
Fig. 23: Undrained Cyclic Simple Shear Test on Monterey #30/0 Sand (Test No. Ms15j)
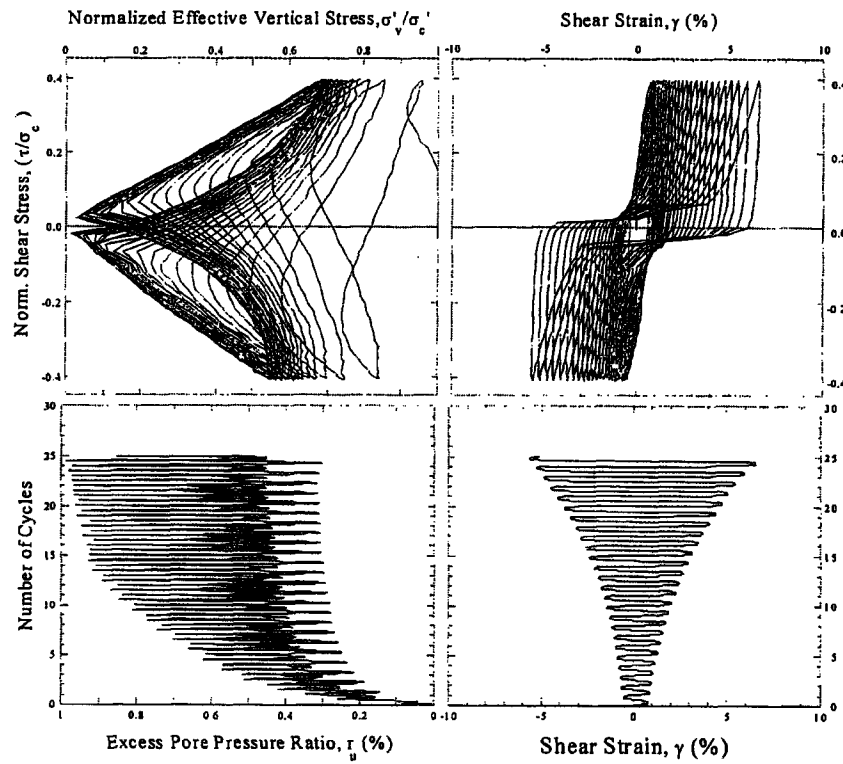Dr=50%, $\sigma_{v,i}$'=85 kPa, CSR=0.22 , α=0

Fig. 24: Undrained Cyclic Simple Shear Test on Monterey #30/0 Sand (Test No. Ms30j)
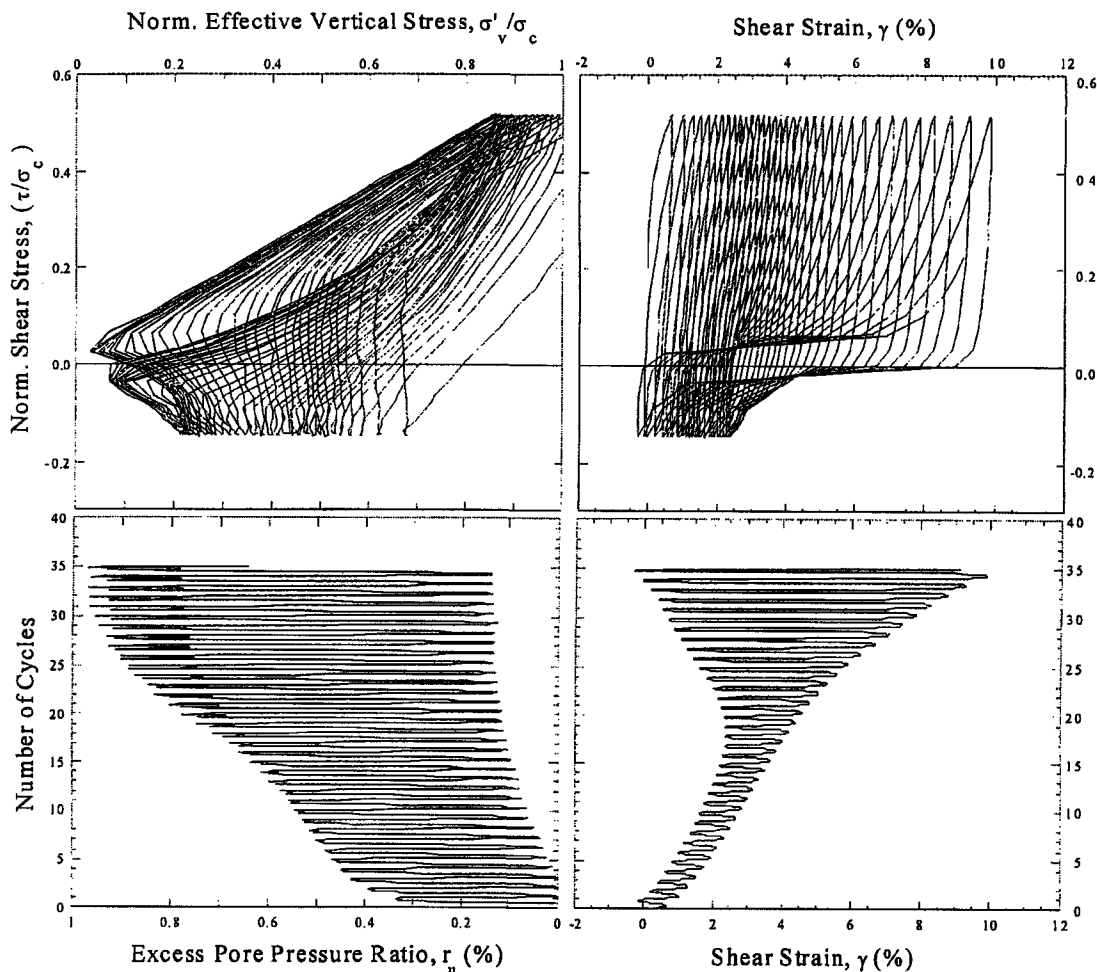Dr=75%, $\sigma_{v,i}$'=85 kPa, CSR=0.4 , α=0

Fig. 25: Undrained Cyclic Simple Shear Test on Monterey #30/0 Sand (Test No. Ms10k)
Dr=55%, $\sigma_{v,i}'$=85 kPa, CSR=0.33 , α=0.18

In addition to the types of cyclic softening and dilatent re-stiffening shown in the two previous figures, this test (Figure 25) also exhibits cyclic "ratcheting" or progressive accumulation of shear strains in the direction of the driving shear force. It is this type of complex "ratcheting" behavior that usually principally controls "small to moderate" liquefaction-induced deformations and displacements (displacements in the range of about 2 to 75 cm. for field cases.)

This problem is further complicated in field cases by the occurrence of cyclic shear stresses "transverse" (not parallel to) the direction of the (static) driving shear stresses. Boulanger et al. (1995) clearly demonstrated that cyclic shear stresses transverse to driving shear forces can, in many cases, represent a more severe type of loading for "triggering" of liquefaction than cyclic shear stresses aligned "parallel" with driving forces. It is only in the last few years, however, that high quality laboratory data with "transverse" as well as "parallel" cyclic simple shear loading (and driving shear

stresses) has begun to be available, and development and calibration of improved analytical and constitutive models for this type of behavior are currently still under development.

Additional complications involved in attempting to predict "small to moderate" liquefaction-induced deformations and displacements include: (1) the irregular and multi-directional loading involved in field situations, representing a complex and multi-directional seismic response problem, and (2) the many types and "modes" of deformations and displacements that can occur.

Figures 26 and 27 illustrate a number of "modes" or mechanisms that can result in "small to moderate" lateral and vertical displacements, respectively. These figures are schematic and for illustrative purposes only; they are not to scale.

Figure 26 illustrates three examples of modes of deformation that can produce "small to moderate" liquefaction-induced

- Liquefied zone

(a) Spreading Towards a Free Face

(b) Spreading Downslope or Downgrade

(c) Localized, Non-directionally Preferential Differential Lateral Displacements
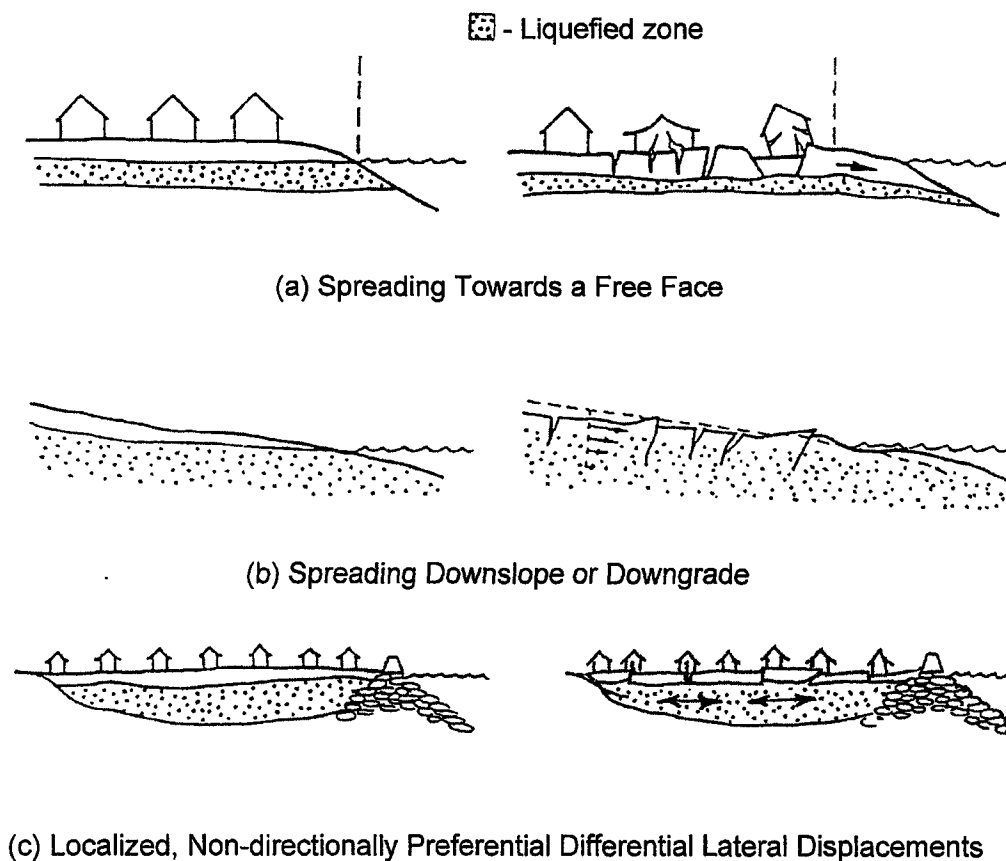
Fig. 26: Schematic Examples of Modes of "Limited" Liquefaction-Induced Lateral Translation

lateral displacements (of less than about 1m.) It should be noted that these can also produce much larger deformations, if the liquefiable soils are very loose, and geometry is sufficiently adverse.

Figure 26(a) shows an example of limited lateral spreading towards a free face, and Figure 26(b) shows an example of limited lateral spreading downslope or downgrade. These modes can also give rise to large displacements, but when the liquefiable soils have limited shear strain potential (the shear strain required for dilatent re-stiffening), then displacements are limited.

Figure 28 (Shamoto, Zhang and Tokimatsu, 1998) presents engineering estimates of limiting (post-liquefaction) shear strains, as a function of SPT N-values. As shown previously in Figures 23 through 25, the shear strain required for dilational re-stiffening decreases with increased initial density (or increased N-value). Although there is not yet a well-established (or well-defined) basis for selection of the precise shear strain corresponding to the "limiting" shear strain (see for examples, Figures 23 through 25), the values of Figure 28 represent suitable approximate values for many engineering purposes. The recommendations of Figure 28 are for sands with approximately 10% silty fines. Shamoto et al. also presented similar figures for 0% and 20% fines, but the differences are less than the uncertainty in defining precisely what is meant by "limiting" shear strain.

(a) Ground Loss Due to Cyclic Densification and/or Volumetric Reconsolidation
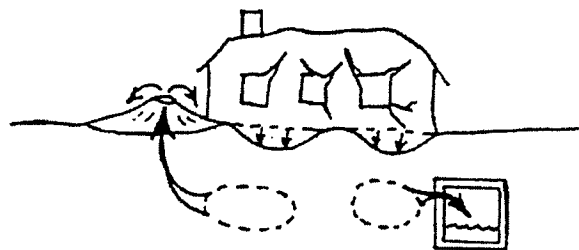
(b) Secondary Ground Loss Due to Erosion of "Boil" Ejecta

(c) Global Rotational or Translational Site Displacement
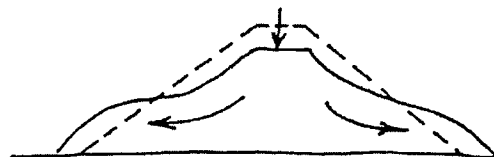
(d) "Slumping" or Limited Shear Deformations
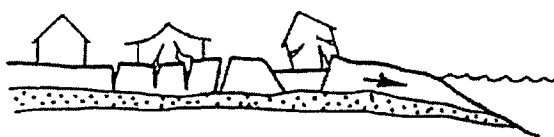
(e) Lateral Spreading and Resultant Pull-Apart Grabens

(f) Localized Lateral Soil Movement

(g) Full Bearing Failure
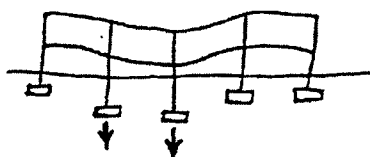
(h) Partial Bearing Failure or Limited "Punching"
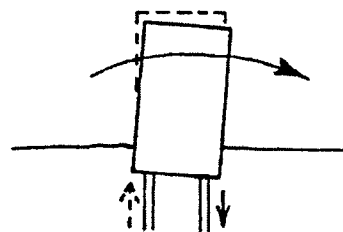
(i) Foundation Settlements Due to Ground Softening Exacerbated by Inertial "Rocking"

Fig. 27: Schematic Illustration of Selected Modes of Liquefaction-Induced Vertical Displacements

Residual shear strain potential

$(\gamma_r)_{max} \rightarrow 50\%$ 20% 10% 5% 2%

Fines (<74 μ)=10%

Shear stress ratio, τ_{av}/σ_z'

Adjusted SPT N-value, N_a

Fig. 28: Recommended Estimates of Limiting Shear Strains for Sandy Soils with ~ 10% Fines (Shamoto et al., 1998)

It should be noted that the N_a-values of Figure 28 correspond to typical Japanese SPT practice, and so should be multiplied (increased) by approximately a factor of 1.1 to develop approximate $N_{1,60,cs}$-values. In addition, as the strains of Figure 28 represent the strains required for re-stiffening in one-half cycle of loading, it must be recognized that multi-cycle "ratcheting" (see for example Figure 25) can produce progressive accumulation of strains with each subsequent cycle. At this time, for moderate to strong seismic loading ($a_{max} \cong 0.025$ to 0.6g), increasing the shear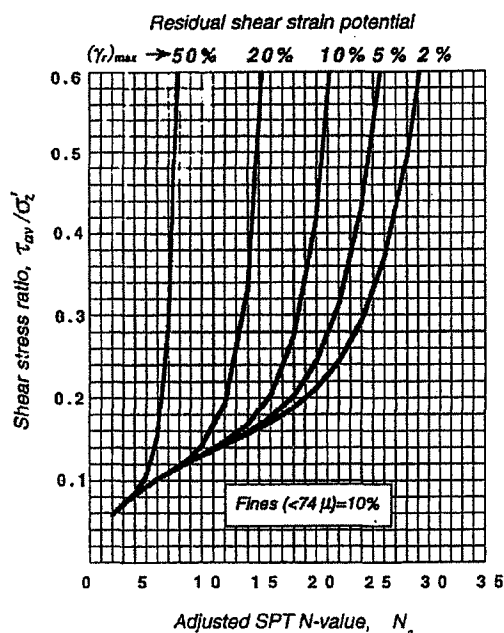 strains of Figure 28 by a factor of about 1.25 to 2.0 to allow for cyclic "ratcheting" appears to provide a conservative basis for engineering estimation of "upper-bound" displacement potential for many cases.

The two general types of lateral spreading deformations illustrated in Figures 26(a) and (b) correspond to the two types of lateral spreading addressed by the empirical corelation proposed by Bartlett and Youd (1995). As shown in Figure 22(a), this approach provided reasonable estimates of expected displacements for cases with displacements of greater than about 2m. However, as shown in Figure 22(b) (which is an enlarged view of part of Figure 22(a)), this approach does not provide accurate or reliable estimates of lateral displacements for cases where measured displacements are less than about 1m. (the range within which complex cyclic inertial loading and cyclic softening and dilational re-stiffening largely control displacements.) Bartlett and Youd have recently futher improved their empirical correlations, but the difficulty in prediction of displacemtns of less than about 1m. persists (Youd, 2000). There are, at present, no well-calibrated and

verified engineering tools for accurate and reliable estimation of lateral displacements in this range. This is an area of urgent need for further advances, and research to fill this gap is underway in several countries.

Figure 26(c) shows another mechanism which can produce "limited" lateral displacements; in this case, liquefaction of soils beneath a non-liquefied surface "crust", and laterally constrained against large lateral spreading towards a free face. When the surface "crust" is thin relative to the thickness of the underlying layer, and when the liquefied soils have low density (low $N_{1,60,cs}$ values), the "crust" can separate into distinct sections or "blocks", and these crustal sections can move differentially with respect to each other. This can produce shearing, compression and tensile separations at the edges of surface blocks. This, in turn, can be damaging to structures and/or utilities that are unfortunate enough to straddle the block boundaries.

There are no good means to predict where the inter-block boundaries will occur, and there are no reliable methods at present to predict the magnitudes of localized differential block displacements that are likely to occur. Ishihara (1985) provides some insight into this "pie crust" problem, as shown in Figure 29. Ishihara suggests, based on empirical observations from a number of Japanese earthquakes, that surface manifestations of liquefaction will not be significant if (1) the site is relatively level, (2) the edges are constrained so that lateral spreading towards a free face is prevented, and (3) the ratio of the thickness of the non-liquefied surface "crust" (H_1) to the thickness of the liquefied underlying soils (H_2) is greater than the values indicated in Figure 29 (as a function of peak ground surface acceleration, as shown.)

Given the potential risk associated with localized differential movements at crustal block boundaries, it is recommended herein that these criteria be supplemented by reinforced and laterally continuous foundations to constrain lateral differential displacements and to reduce differential vertical displacements at the bases of structures at such sites, especially when the liquefied layer contains soils with low equivalent $N_{1,60,cs}$ values ($N_{1,60,cs} \leq 15$), or when the ratios of H_1/H_2 are near the boundaries of Figure 29.

In addition to differential lateral displacements, engineers must also deal with the hazard associated with both total and differential potential vertical displacements. There are a number of mechanisms that can produce vertical displacements of sites and/or structures and other engineered facilities. Figure 27 presents schematic illustrations of a number of these. Again, this figure is schematic and for illustrative purposes only; it is not to scale. The modes of vertical displacement illustrated in Figure 27 can be grouped into three general catagories. Figures 27(a) and (b) illustrate settlements due to reduction or loss of soil volume. Figure 27(c) through (f) illustrate modes of settlement due to deviatoric ground movements. Figures 27(g) through (i) illustrate structural settlements due to full or partial bearing failures.
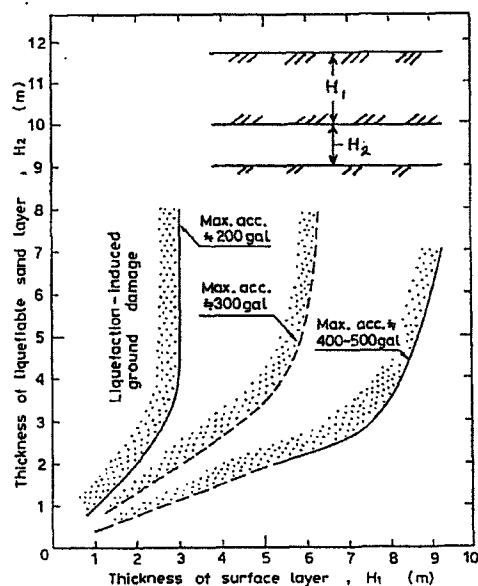
Fig. 29: Proposed Boundary Curves for Site Indentification of Liquefaction-Induced (Surface) Damage.

Figure 27(a) shows "ground loss" or settlement due to cyclic densification of non-saturated soils and/or due to volumetric reconsolidation of liquefied (or partially liquefied) soils as cyclically-induced pore pressures escape by drainage. The overall magnitude of these types of settlements can be reasonably well predicted by several methods (e.g.: Tokimatsu and Seed, 1984: Ishihara and Yoshimine, 1990), but these methods cannot reliably predict the magnitude and distribution of locally differential settlements. Overall settlement estimates are generally accurate within $\pm$ 50 to 70%, so long as suitable adjustments are made for fines content (as both methods are for "clean" sands.) The fines adjustment recommended here is that of Equations 6 and 7.

Figure 27(b) illustrates a second mechanism of ground loss; secondary ground loss as a result of erosion of soil particles carried by water escaping through cracks and fissures (often referred to as "sand boils") as excess pore pressures are dissipated. Boil ejecta (transported soils) can be carried to the ground surface, or they can be carried to accessible buried voids (e.g.: basements, buried culverts and sewers, etc.) Secondary ground loss due to erosion of boil ejecta is usually localized, and so can be locally differential. It is also essentially impossible to predict. The best defense here is usually to ensure sufficient lateral continuity of foundations as to be able to "bridge" or cantilever over localized subsidences. Another alternative is deep foundation support (piles or piers) extending beneath the depth of potential ground loss.

Figures 27(c) and (d) illustrate rotational and "slumping" (distributed shear) types of ground movements that produce settlements at the crests or heels of the slopes or embankments. Although these types of potential liquefaction-induced deformations and displacements are relatively amenable to engineering prediction when they are "large" (>1m.), there are at present no accurate and reliable (or well-calibrated) methods for estimation of expected displacements when displacements will be small to moderate (D $\cong$ 0.05 to 0.75m.) Accordingly, significant judgement is currently required to assess the likely deformations, and their impact on structures and other engineered facilities. The lack of reliable and well-calibrated analysis tools here often results in the need for conservative assumptions, and often leads to implementation of conservative hazard mitigation measures.

Figures 27(e) and (f) illustrate closely related mechanisms that can produce surface settlements. Figure 27(e) illustrates lateral spreading producing grabens, or settlements, in zones of locally differential extension (pull-apart zones). Figure 27(f) illustrates localized lateral soil movement producing both heaving and settlement as overall soil volume is largely conserved. These types of potential movements are also difficult to predict, and again conservative assumptions and/or conservative steps to mitigate this type of hazard are often called for when these types of movements are judged to represent potentially serious hazards for a site, structure, or other engineered facility.

Finally, in addition to liquefaction-induced soil (or site) displacements, another class of potential concerns are those associated with potential differential movements of structures relative to the ground. Figures 27(g) through (i) illustrate several subsets of these types of movements.

Figure 27(g) represents the case in which liquefaction-induced loss of strength and stiffness is sufficiently severe that full bearing failure occurs. This type of full bearing failure occurs when overall bearing capacity, based on post-liquefaction strengths ($S_{u,r}$) as appropriate, is insufficient for static equilibrium under gravity loading. This can produce very large "punching" settlements (many tens of centimeters or more), and can even lead to toppling of structures when they are narrow relative to their height.

Figure 27(h) represents partial bearing failure or limited "punching" settlements. These limited punching types of settlements can occur at isolated footings, or can occur with mat and raft foundations (especially at corners and edges.) Limited punching settlements are generally associated with situations in which post-liquefaction strengths are sufficient to prevent full bearing failure, and they are the result of cyclic softening and attendant deformations required to generate sufficient dilational re-stiffening as to arrest movements. Estimation of these "limited" punching/bearing settlements can be further complicated by the interaction of increased cyclic vertical loads due to inertial "rocking" of structures with cyclic softening (and cyclic dilational re-stiffening), as illustrated schematically in Figure 27(i). There are, at present,

no reliable and well-calibrated engineering/analytical tools for estimation of likely limited punching settlements. This is a major gap in practice, as it is limited punching settlements (in the range of about 0.05 to 0.75 m.) that represent one of the principal liquefaction-related hazards for many buildings and engineered structures.

Widespread liquefaction in the city of Adapazari in the recent 2000 Kocaeli (Turkey) Earthquake produced differential foundation/soil punching types of settlements in this range for hundreds of buildings, and many additional buildings suffered similar ranges of settlements in the cities of Wu Feng, Nantou, and Yuan Lin during the 2000 Chi Chi (Taiwan) Earthquake. These two events thus provided both strong incentive, as well as large numbers of potential field case histories, and as a result considerable research efforts are currently underway to develop methods for estimation of these types of "limited" punching/bearing displacements.

In the interim, it is noted that punching/bearing settlements can be expected to be "large" (many tens of centimeters, or more) when post-liquefaction strengths provide a Factor of Safety of less than 1.0 under gravity loading (without additional vertical loads associated with earthquake-induced "rocking", etc.) Similarly, these types of punching/bearing settlements can be expected to be "small" (less than about 3 to 5 cm.) when liquefaction occurs, but the minimum Factor of Safety under the worst-case combination of seismically-induced (transient) vertical loads plus static (gravity) loads, and based on post-liquefaction strengths ($S_{u,r}$), is greater than about 2.0.

ASSESSMENT OF THE CONSEQUENCES OF LIQUEFACTION-INDUCED DEFORMATIONS AND DISPLACEMENTS

There is an urgent need for improvement of our ability to accurately and reliably estimate expected "limited", or "small to moderate" liquefaction-induced deformations and displacements. There is a similar need to improve our ability to assess the expected ramifications of these types of displacements and deformations on the performance of buildings and other engineered facilities. In addition, there are currently no well-established standards regarding expectations of "acceptable" performance for most types of structures and facilities. These are all important areas in which further progress is urgently needed.

During the middle portion of the 20th Century, considerable research was done to develop an understanding of the consequences of various levels of differential (static) settlements on different types of structures. This work, which involved considerable field studies of performance of actual structures, also required close collaboration between geotechnical and structural professionals. The results of these studies led to greatly improved understanding of the ramifications of various levels of differential (static)

settlements, establishment of accepted standards of practice and performance, and codification of these types of standards.

Similar efforts are now needed with respect to development of methods for assessment of the structural consequences of liquefaction-induced differential lateral and vertical displacements, as well as for determination of "acceptable" levels of resultant structural performance. Levels of differential structural displacements representing adequate structural performance in a "life safety" context are not well established. As we move inexorably towards "performance based" seismic engineering design, increasingly refined predictions of structural performance in the event of various levels of structural displacement will be needed, and increasingly challenging decisions (and standards) will be needed regarding "acceptable" levels of performance with regard to preserving repairability, reducing overall damages, maintaining serviceability and/or minimizing out of service duration, etc.

The widespread liquefaction-induced damages to hundreds of structures in both the recent Koaceli (Turkey) and Chi Chi (Taiwan) Earthquakes provide both incentive, and large field performance laboratories, with which to begin this process. In the interim, engineers are left without strong guidance, and considerable engineering judgement is required.

MITIGATION OF LIQUEFACTION HAZARD

When satisfactory performance of structures and/or other engineered facilities cannot adequately reliably be assured, engineered mitigation of the unacceptable liquefaction hazard is generally required. There are many methods, and variations on methods, currently available for this, and more are under development.

Table 2 presents a brief list of selected major mitigation methods available. It should be noted that these do not have to be employed singly; it is often optimal to use two or more methods in combination.

It is not reasonable, within the constraints of this paper, to attempt a comprehensive discussion of all available mitigation methods. Instead, limited comments will be offered regarding various aspects of some of these. It should be noted that mitigation of liquefaction hazard is an area subject to considerable controversy, and that our understanding of the efficacy of some of these methods is still evolving. It is suggested that key issues to be considered in selection and implementation of mitigation methods are: (1) applicability, (2) effectiveness, (3) the ability to verify the reliability of the mitigation achieved, (4)cost, and (5) other issues of potential concern (e.g.: environmental and regulatory issues, etc.).

More comprehensive treatments of many of the mitigation methods listed in Table 2 are available in a number of refeences (e.g.: Mitchell, 1995; Hausmann, 1990).

Table 2: List of Selected Methods for Mitigation of Seismic Soil Liquefaction Hazard

General Category	Mitigation Methods	Notes
I. Excavation and/or compaction	(a) Excavation and disposal of liquefiable soils (b) Excavation and recompaction (c) Compaction (for new fill)	
II. In-situ ground densification	(a) Compaction with vibratory probes (e.g.: Vibroflotation, Terraprobe, etc.) (b) Dynamic consolidation (Heavy tamping) (c) Compaction piles (d) Deep densification by blasting (e) Compaction grouting	-Can be coupled with installation of gravel columns -Can also provide reinforcement

III. Selected other types of ground treatment	(a) Permeation grouting
	
	(b) Jet grouting
	
	(c) Deep mixing
	
	(d) Drains
	  - Gravel drains
	  - Sand drains
	  - Pre-fabricated strip drains
	
	(e) Surcharge pre-loading
	
	(f) Structural fills
		-Many drain installation processes also provide in-situ densification.

IV. Berms, dikes, sea walls, and other edge containment structures/systems	(a) Structures and/or earth structures built to provide edge containment and thus to prevent large lateral spreading	
V. Deep foundations	(a) Piles (installed by driving or vibration) (b) Piers (installed by drilling or excavation)	-Can also provide ground densification
VI. Reinforced shallow foundations	(a) Grade beams (b) Reinforced mat (c) Well-reinforced and/or post-tensioned mat (d) "Rigid" raft	

The first class or catagory of methods listed in Table 2 involve surface compaction. When this is the case, potentially liquefiable soil types should be placed in layers and compacted, using vibratory compaction, to specifications requiring not less than 95% relative compaction based on the maximum dry density ($\gamma_{d,max}$) as determined by a Modified AASHTO Compaction Test (ASTM 1557D).

The second group of methods listed in Table 2 involve in-situ ground densification. It is recommended that these methods be coupled with a suitably comprehensive post-treatment verification program to assure that suitable mitigation has been achieved. CPT testing is particularly useful here, as it is rapid and continuous. When CPT is to be used for post-densification verification, it is a very good idea to establish pre-densification CPT data, and to develop site-specific cross-correlation between SPT and CPT data.

In addition, it should be noted that ageing effects (including establishment of microbonding and even cementation at particle contacts) is disrupted by in situ densification. These ageing effects increase both resistance to liquefaction, and also resistance to penetration (as measured by SPT, CPT, etc.) Immediately after in-situ densification, despite increased overall density of the soils, it is not unusual to find that penetration resistances have not increased nearly as much as expected, and in some cases they have even been observed to decrease slightly. Over subsequent weeks and months, however, as ageing effects re-establish themselves, penetration resistances generally continue to increase. A large fraction of ageing effects usually occur over the first 6 to 12 weeks after treatment, and penetration tests performed sooner than this can be expected to provide conservatively biased results.

In-situ vibrodensification, or compaction by means of vibratory probes, has been employed to depths of 70m. Difficulties in penetrating to depth through dense and/or coarse soils, and failure to deliver sufficient vibrational energy as to achieve adequate densification in the face of high overburden stresses, can limit the efficacy of these methods at the deepest of these depths.

Vibrodensification is generally effective in soils with less than about 5% clay fines, but can be ineffective in soils with larger fractions of clay fines. It had long been thought that the diffficulty in vibrodensification of soils with high fines contents was related to the inability of water to escape, and indeed some improvement in densification of soils with high fines contents has been observed with the use of wick drains to assist in allowing egress of water. It is noted, however, that the clay contents at which vibrodensification begins to be ineffective are very similar to the clay contents at which classic cyclically-induced liquefaction ceases to occur (see Figure 2). It appears likely that, as vibrodensification essentially works by liquefying and densifying the soils, the limit of "treatable" soil types is largely coincident with the types of soils that are "liquefiable", and thus in need of treatment.

Some of the vibrodensification methods also result in installation of dense gravel columns through the treated ground. It has been suggested that these dense gravel columns, which have high shear moduli relative to the surrounding (treated) soils, will attract a large share of the shear stresses propagating through the composite treated ground, and thus partially shield the softer surrounding soils. This, in turn, would produce the added benefit of reducing he cyclic shear stress ratios (CSR) to which the treated soils would be subjected during an earthquake.

Estimates of the level of shear stresses borne by the dense gravel columns are sometimes computed by estimating the contributions of the stiffer columns and the softer surrounding soil, based an assumption of a simple shear mode of deformation, and using contributory areas of the gravel columns and the surroundiing soils and their respective shear moduli. Unfortunately, for column height to diameter ratios of greater than about three, the deformations of the gravel columns are dominated by flexure, rather than simple shear, and this renders them much softer than the above-described analyses would suggest. Indeed, the gravel columns generally provide relatively little "shielding" of the surrounding soils, and this hypothesized shielding effect can conservatively be neglected.

Dynamic consolidation (or heavy tamping) involves raising a large mass to great height (with a crane), and then dropping it, producing both impact and vibrational compaction. The depth to which this can be effective is principally a function of the weight that can be raised, and the height from which it can be dropped. Good results can usually be achieved to depths of up to about 7 to 10m. with "conventional" equipment, and special purpose equipment has been built to extend these depths somewhat for individual, large projects. Dynamic consolidation is generally less expensive (per treated volume) than vibrodensification, but cannot reach the same depths and is progressively less effective as depth increases. Other issues, including treatable soil types and post-treatment verification (including ageing effects) are largely as discussed previously for vibrodensification.

Compaction piles provide improvement by three mechanisms; (1) by densification due to driving installation, (2) by increasing lateral stresses, and (3) by providing structural reinforcing elements. This method is only rarely used, however, due to its cost. It is generally employed in unusual situations where other methods cannot reliably be implemented.

Blasting can be used to achieve deep densification of potentially liquefiable soils. This method, however, tends to produce less uniform densification than vibrodensification, and generally cannot reliably produce densities as high as those that can be obtained with high energy vibrodensification methods that effectively transmit high vibrational energy to soils at depth (e.g. Vibroflotation, etc.) Blasting also raises environmental concerns, issues regarding propagation of vibrations across neighboring sites, and issues regarding noise and safety.

Compaction grouting is the last of the "in-situ ground densification" methods listed in Table 2, and also the first of three "grouting" methods listed in Table 2. Compaction grouting involves injection of very stiff (low slump) cement grout into the ground at very high pressure, ideally forming "bulbs" of grout and displacing the surrounding soils. Compaction grouting works both by densifying soils, and by increasing in-situ effective lateral stresses. The degree of densification that can be achieved by the monotonic (non-cyclic) loading imposed by the growing grout mass is dilationally limited, however, and recent research suggests that the increased lateral stresses can relax over time. An additional drawback is the difficulty in verifying improvement by means of penetration testing. Compaction grouting performed well at one site in San Francisco during the 1989

Loma Prieta Earthquake, but the site was subjected to only moderate levels of shaking ($a_{max} \sim 0.2g$., and a relatively short duration of shaking). This method remains unproven at higher levels of shaking.

Permeation grouting involves injection of a grouting agent in a fluid form into the void spaces between the soil grains. A limitation of this method is the inability of even the most finely ground cement grouts to reliably penetrate into the voids of soils with greater than about 6 to 10% fines. As this can include silty fines, this leaves most silty soils potentially vulnerable to liquefaction. This is also problematic in sandy and silty soil deposits of variable fines content, a common situation. Chemical grouts are available that can more reliably penetrate into finer soils, but these are increasingly problematic with regard to environmental and regulatory issues. Another significant drawback with permeation grouting is the inability to know, with certainty, just where the grout has actually gone. This exacerbated by the inability to "check" conditions after treatment, except by means of expensive borings, as the hardened grout impedes penetration of CPT. Finally, cost is very high.

Jet grouting is an attempt to achieve grout penetration by jetting at very high pressure from a rotating probe, as the probe is withdrawn. Ideally, this produces a cylindrical column of treated soil (or soil cement). Penetration of the jet varies with soil density and character, however, so that the diameter of the treated column can be uncontrollably variable. Coarse particles (gravelly and coarser) can fully deflect the jet, leaving untreated slivers in the treated column. As with permeation grouting, post-treatment "checking" is rendered difficult and expensive by the hardened treated column. This method is also expensive, and it is not economical to attempt to treat he full volume of liquefiable soil. Accordingly, treatment of overlapping columns is employed, as described below for deep soil mixing. Overall, jet grouting is an uncertain process, and has largely been supplanted by the more certain process of deep mixing.

Deep mixing involves the use of large augers both to introduce cement grout and to mix it with the soil, producing treated soil cement columns. This is essentially a brute force method, and it has a significant advantage over both permeation and jet grouting inasmuch as the injection and mixing process provides reliable treatment of a known volume of soil. The problem with deep mixing is that it is not economical to treat the full liquefiable soil volume. Accordingly, rows of slightly overlapping treated columns are used to create "walls", and these are arranged in a cellular pattern (in plan), surrounding "cells" of untreated soil. The soils within the cells can still liquefy, however, especially when the "treatment ratio" (the ratio between treated soil volume, and the untreated volume within the cells) is low. Soils within the cells can also settle, producing differential settlements. This can, clearly, be an effective method, and performance was good at one site during the recent 1995 Kobe Earthquake. It is not known with any assurance, however, exactly what treatment ratios are required for various situations, and as the cost of treatment is relatively high, selection of treatment ratios has a tremendous impact on overall cost.

Drains are a very interesting and challenging method for mitigation of liquefaction hazard. An important potential drawback of this method is that it poses a "brittle" solution; it is effective only if it successfully promotes sufficiently rapid dissipation of pore pressures as to prevent the occurrence of liquefaction. If pore pressure dissipation is not sufficiently rapid during the relatively few critical seconds of the earthquake, however, this method does relatively little to improve post-liquefaction performance. An additional drawback is that, although it may prevent liquefaction, this method only reduces (but does not eliminate) settlements due to cyclic densification and reconsolidation after partial cyclic pore pressure generation.

A major difficulty in the use of drains is the need to assess the in-situ permeability of the soils to be drained. It is usually difficult to reliably assess the in-situ permeability of soils with an assured accuracy of better than about plus and minus one to two orders of magnitude, and this type of uncertainty can have a tremendous effect on the required spacing of drains. This is routinely exacerbated by the intrinsic in-situ variability in character (e.g.: fines content, etc.) of liquefiable soil deposits. It should also be noted that concerns regarding potential "plugging" of drains, either by formation of an external "skin" of transported fines, or by infiltration of transported fines into soil drains, is a risk that is difficult to quantify. When drains are installed by vibro-probes, without external filters, significant mixing of the coarse (and ostensibly free draining) drain soils and the (finer) surrounding soils routinely occurs, and this greatly reduces the drains' ability to rapidly pass large volumes of water over the critical few seconds of an earthquake.

Drains, alone, can represent a difficult and uncertain mitigation approach. Many of the drain installation techniques employed also provide in-situ vibrodensification, however, and this can be a very attractive combination. As discussed previously, in-situ vibrodensification can be an effective mitigation method, and can be checked to verify post-treatment conditions. When coupled with drains, the drains can be useful in retarding the formation of "loose" zones and/or water blisters at the interfaces between layers of differing vertical permeabiltiy.

Surcharge pre-loading (Method III(e) in Table 2) induces increased vertical and horizontal effective stresses. When the surcharge is then removed, the resulting overconsolidation leaves the soil somewhat more resistant to triggering or initiaion of liquefaction. The degree of increased liquefaction resistance that can be achieved is only moderate, however, and this is not generally an effective method in regions of high seismicity.

Structural fills can be used to increase the thickness of a non-liquefiable "crust" overlying potentially liquefiable soils (see Figures 26(c) and 29). These can be further improved by

inclusion of horizontal layers of high-strength and ductile reinforcing mats, to minimize differential movements at the edges of "blocks" of intact crust and/or structural fill (see Figure 26(c)).

Structural fills can also be used to buttress free faces towards which lateral spreading otherwise might occur, and this leads naturally to the suite of methods in Group IV of Table 2. These methods involve creating secure containment of "edges" or free faces towards which liquefaction-induced lateral spreading might otherwise occur. The key here, of course, is to ensure that the containment system itself does not fail during the earthquake. This can only prevent "large" lateral spreading deformations; it usually does little to reduce localized differential lateral and vertical movements and/or bearing settlements.

The next two groups of mitigation methods in Table 2 are "structural" methods, and the first of these is the use of deep foundations (piles or piers). Piles or piers, safely bearing at depths below the occurrence of liquefaction (or significant cyclic softening due to partial liquefaction), can provide reliable vertical support and so can reduce or eliminate the risk of unacceptable liquefaction-induced settlements. Pile or pier foundations do not, however, necessarily prevent damages that may occur as a result of differential lateral structural displacements, so piles and/or piers must be coupled with sufficient lateral structural connectivity at the foundation as to safely resist unacceptable differential lateral displacements.

An additional concern, which prior to this past decade had been routinely neglected, is the need to ensure that the piles or piers themselves are not unacceptably damaged during seismic excitation. Numerous field cases of damage to piles during earthquakes, dating back as far as the 1964 earthquakes in Alaska and Niigata (Japan), and continuing through the recent Kobe (Japan) and Chi Chi (Taiwan) Earthquakes, continue to emphasize the importance of this. Significant research efforts over the past 15 years have led to the development of a range of analytical methods for this problem, ranging from fully nonlinear, time domain, fully integrated soil/pile/ superstructure interaction analyses to considerably simpler analyses based on separate assessment of expected site response and resultant pile (or pier) loadings (Pestana, 2001). These types of methods, complemented with appropriate conservatism, can provide a suitable basis for analysis of this issue, and for the design and detailing of piles (or piers) and pile/cap connections.

The second group of "structural" mitigation methods in Table 2 involve the use of reinforced shallow foundations to resist differential lateral and vertical displacements. Japanese practice has increasingly employed both grade beams and continuous reinforced foundations for low to moderate height structures, and performance of these types of systems in earthquakes has been good. The strength and stiffness of both grade beams and reinforced continuous foundations used in Japan for this purpose are higher than those often used in U.S. practice, however, and standards for design of these are

lacking in the U.S., so that engineering judgement is required here.

The final group of mitigation options in Table 2 is self-explanatory.

BRIEF COMMENTS ON ADVANCES IN ASSESSMENT OF SEISMIC SITE RESPONSE

Over the past decade, the topic of site-specific seismic site response has evolved from an issue of controversy to a well-accepted principle addressed in most up to date seismic building codes. This very rapid evolution was driven, in large part, by the important lessons provided by the 1985 "Mexico City", 1989 Loma Prieta, 1994 Northridge and 1995 Hyogoken-Nanbu (Kobe) Earthquakes, and by the large and unprecedented amounts of strong motion data recordings provided by these important events.

Spurred by this, significant advances have occurred in both research and practice. The treatments of site response issues in recent seismic code provisions in both the U.S. and Japan represent a major step forward, and similar treatments are appearing around the world. Analytical and modelling capabilities are also advancing rapidly. Coupled with the strong motion data necessary to refine and calibrate them, these now provide powerful and increasingly accurate and reliable tools for engineering analysis of seismic site response. Understanding of seismic soil properties and response characteristics, and understanding of seismological issues affecting seismic site response have also advanced considerably.

Given the length constraints, and the treatment already afforded liquefaction-related issues, it will not be possible to attempt a comprehensive treatment of seismic site response issues within this paper. Instead, comments will be offered on selected issues affecting engineering assessment of seismic site response in earthquake engineering practice.

Table 3, and Figures 30 and 31, present a slight modification and updating of the empirical categorization of sites for site response assessment purposes presented by Seed et al. (1997). (Modifications of the suggested site classifications in Table 3 relative to the earlier publication are minor; the principal difference is that the recommended response spectral shapes of Figure 31 have been re-cast to show "mean" rather than mean plus one-half standard deviation values.)

Table 3 presents a recommended system for classification of sites for purposes of site response evaluation. Similar, but simplified, systems are currently used in the 1994 NEHRP and 1996 UBC seismic code provisions. This classification system is more detailed than most engineers are used to, and is instructive in many regards.

Table 3: Proposed Site Classification System for Seismic Site Response

Site Class	Site Condition	General Description	Site Characteristics
(A_0)	A_0	Very hard rock	V_s(avg.)>5,000 ft/s in top 50 ft.
A	A_1	Competent rock with little or no soil and/or weathered rock veneer.	$2,500$ ft/s $\leq V_s$(rock) $\leq 5,000$ ft/s, and $H_{soil+weathered\ rock} \leq 40$ ft, with $V_s > 800$ ft/s (in all but the top few feet[3])
AB	AB_1	Soft, fractured and/or weathered rock.	For both AB_1 and AB_2: 40 ft $\leq H_{soil+weathered\ rock} \leq 150$ ft, and $V_s > 800$ ft/s (in all but the top few feet[3])
	AB_2	Stiff, very shallow soil over rock and/or weathered rock.	
B	B_1	Deep, primarily cohesionless[4] soils. ($H_{soil} \leq 300$ ft.)	No "soft clay" (see note 5), and $H_{cohesive\ soil} > 0.2\ H_{cohesionless\ soil}$
	B_2	Medium depth, stiff cohesive soils and/or mix of cohesionless with stiff cohesive soils; no "soft clay".	$H_{all\ soils} \leq 200$ ft, and V_s (cohesive soils) > 600 ft/s (see Note 5)
C	C_1	Medium depth, stiff cohesive soils and/or mix of cohesionless with stiff cohesive soils; thin layer(s) of soft clay.	Same as B_2 above, except 0 ft $< H_{soft\ clay} \leq 10$ ft. (see Note 5)
	C_2	Very deep, primarily cohesionless soils.	Same as B_1 above, except $H_{soil} > 300$ ft.
	C_3	Deep, stiff cohesive soils and/or mix of cohesionless with still cohesive soils; no "soft clay".	$H_{soil} > 200$ ft., and V_s (cohesive soils) > 600 ft/s
	C_4	Soft, cohesive soil at small to moderate levels of shaking.	10 ft $< H_{soft\ clay} \leq 90$ ft, and $A_{max,rock} \leq 0.25$ g
D	D_1	Soft, cohesive soil at medium to strong levels of shaking.	10 ft $< H_{soft\ clay} \leq 90$ ft, and 0.25 g $< A_{max,rock} \leq 0.45$ g, or (0.25 g $< A_{max,rock} \leq 0.55$ g and M $\leq$ 7-1/4)
$(E)^6$	E_1	Very deep, soft cohesive soil.	$H_{soft\ clay} > 90$ ft (see Note 5)
	E_2	Soft, cohesive soil and very strong shaking.	$H_{soft\ clay} > 10$ ft and either: $A_{max,rock} > 0.55$ g or $A_{max,rock} > 0.45$ g and M > 7-1/4
	E_3	Very high plasticity clays.	$H_{clay} > 30$ ft with PI $> 75\%$ and $V_s < 800$ ft/s
$(F)^7$	F_1	Highly organic and/or peaty soils.	H > 10 ft of peat and/or highly organic soils.
	F_2	Sites likely to suffer ground failure due either to significant soil liquefaction or other potential modes of ground instability.	Liquefaction and/or other types of ground failure analysis required.

Notes:

1. H = total (vertical) depth of soils of the type or types referred to.
2. V_s = seismic shear wave velocity (ft/s) at small shear strains (shear strain ~ $10^{-4}\%$).
3. If surface soils are cohesionless, V_s may be less than 800 ft/s in top 10 feet.
4. "Cohesionless soils" = soils with less than 30% "fines" by dry weight. "Cohesive soils" = soils with more than 30% "fines" by dry weight, and 15% $\leq$ PI (fines) $\leq 90\%$. Soils with more than 30% fines, and PI (fines) < 15% are considered "silty" soils herein, and these should be (conservatively) treated as "cohesive" soils for site classification purposes in this Table.
5. "Soft Clay" is defined as cohesive soil with: (a) Fines content $\geq$ 30%, (b) PI(fines) $\geq$ 20%, and (c) $V_s \leq 600$ ft/s.
6. Site-specific geotechnical investigations and dynamic site response analyses are strongly recommended for these conditions. Response characteristics within this Class (E) of sites tends to be more highly variable than for Classes A_0 through D, and the response projections herein should be applied conservatively in the absence of (strongly recommended) site-specific studies.
7. Site-specific geotechnical investigations and dynamic site response analyses are *required* for these conditions. Potentially significant ground failure must be mitigated, and/or it must be demonstrated that the proposed structure/facility can be engineered to satisfactorily withstand such ground failure.

Figures 30 and 31 compliment Table 3, and provide a basis for empirical assessment of response for the site categories of this table. Figure 30 presents "mean" estimates of peak ground surface amplification, relative to competent rock (Class A) sites. Figure 31 presents recommended simplified elastic acceleration response spectra (5% damping) for the various site classes in Table 3. Used together, Figures 30 and 31 provide general estimates of the mean ground surface acceleration and response spectral values for the recommended site classes. First-order estimates of the mean plus one standard deviation values can be obtained by simply multiplying the resulting values (both a_{max} and all spectral values, S_A) by about 1.3.

It should be noted that most attenuation relationships for "rock" motions do not, in fact, represent "rock" sites, as defined in Table 3, but are instead based largely on data from "near rock" sites (Site Class AB in Table 3), with resultant attenuation-based "rock" estimates of $a_{max,rock}$ representing a condition somewhat intermediate between Classes A and AB, but generally closer to AB. Accordingly, it is recommended that attenuation-based predictions of $a_{max,rock}$ (from "most" attenuation relationships developed for active seismic regions) be reduced by 10 to 15%, then treated as approximate "rock" values (Class A) in using Figure 30.

The amplification predictions of Figure 30 are intended as "mean" values, and it is important to understand the variance possible as different site conditions interact with different excitation motions. Figure 32 provides a good illustration of this type of variability. This figure shows amplification ratios calculated (based on fully nonlinear and "equivalent linear" site response analyses), as well as recorded data, for deep cohesive sites corresponding largely to those of Class C_3 in Table 3 (Chang et al., 1997). As shown in this figure, variance can be significant.

Similarly, Figure 33 shows both calculated and recorded response spectral shapes (5% damped) for sites largely corresponding to Class C sites (mainly C_2 and C_3 sites). Again, variance is significant.

A major drawback of this, and any system for estimation of likely site response based on "averaging" of calculated and/or observed values for "similar" sites, is the failure to recognize the fact that "similar" sites are not the same. Each individual site has its own characteristics, and will interact with incoming strong motions in its own way. By averaging the response performance of a "group" of sites (and for a suite of varying input or incoming motions), the individual peaks in a spectral response are statistically leveled, reducing the individual site response to the "average" across the group. This can be unconservative.

Peaks in response spectra are very important when they interact adversely with the structure or facility under design consideration. When the predominant period of the ground motion occurs near, and slightly to the right of, the period associated with strong resonant response of a structure (or other engineered system), the structure tends to "walk into" resonant interaction with these motions as it softens and begins to sustain damage. When the predominant period of the ground motion occurs near, but to the left of, the resonant period of the structure, however, softening of the structure can allow it to "walk away" from resonant interaction with these motions. The "peaks" of surface response spectra, and their periods, can be very important. Unfortunately, these "peaks" are lost in any group-averaging scheme.

For most sites, a fairly good estimate of the elastic predominant (first mode) site period can be made as

$$T_{p,elastic} \approx \frac{4H}{V_s^*} \qquad \text{(Eq. 15)}$$

Where H is the depth to strong, competent material (material with $V_s > 2,500$ ft/s), and V_s^* is the equivalent overall shear wave velocity (from the ground surface to this depth, H) taken by inverting the shear wave travel time (t_H) over this depth range as

$$t_H = \sum \left(\frac{h_i}{V_{s,i}} \right) \qquad \text{(Eq. 16(a))}$$

$$V_s^* = \frac{H}{t_H} \qquad \text{(Eq. 16(b))}$$

where h_i = the thickness of each sub-stratum and $V_{s,i}$ = the shear wave velocity within the sub-stratum.

For sites with complex layering and strong impedance transitions, Equations 15 and 16(a) can over-estimate $T_{p,elastic}$ and higher-order methods are required. The venerable equivalent linear site response analysis program "SHAKE", for example, in all of its current versions, will directly calculate $T_{p,elastic}$ for any given horizontally layered profile. $T_{p,elastic}$ can also be measured directly using microtremor or low level aftershock motions.

$T_{p,elastic}$ is the small strain site period, and is not the predominant site period that will be operative at higher levels of earthquake shaking. The "softened" representative predominant site period at stronger levels of shaking is a complex function of interactions between excitation motions and site properties (e.g.: stratigraphy, nonlinearity of properties, etc.). An approximate estimate of T_p can be made as

$$T_{p,earthquake} \approx T_{p,elastic} \left[(1 + \frac{a_{max}}{3}) \text{ to } (1 + \frac{a_{max}}{1}) \right]$$
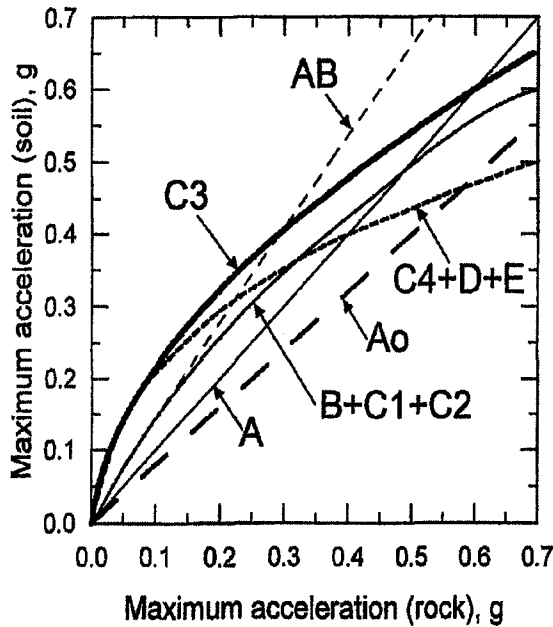
$$\text{(Eq. 17)}$$

Fig. 30: Proposed Site-Dependent Relationship Between mean a_{max} and a_{max} for "Competent Rock Sites (Seed et al., 1997)
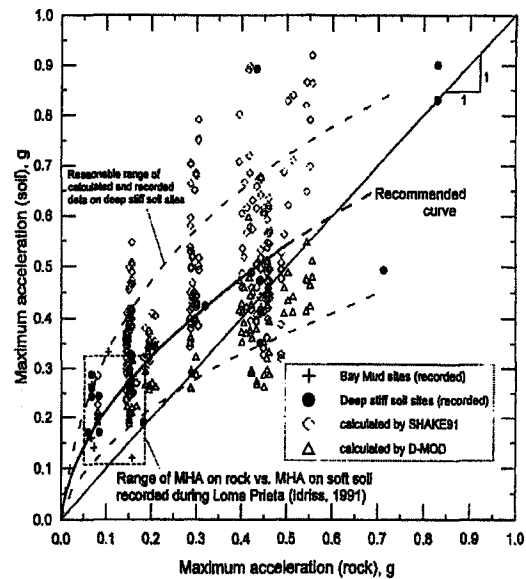

Fig. 32: Relationship for a_{max} or $a_{max,rock}$ for Deep Stiff Soil Sites Based on Available Empirical Data from the Loma Prieta and Northridge Earthquakes and Calculations Using Both Equivalent Linear and Fully Nonlinear Site Response Methods (Chang et al., 1997)
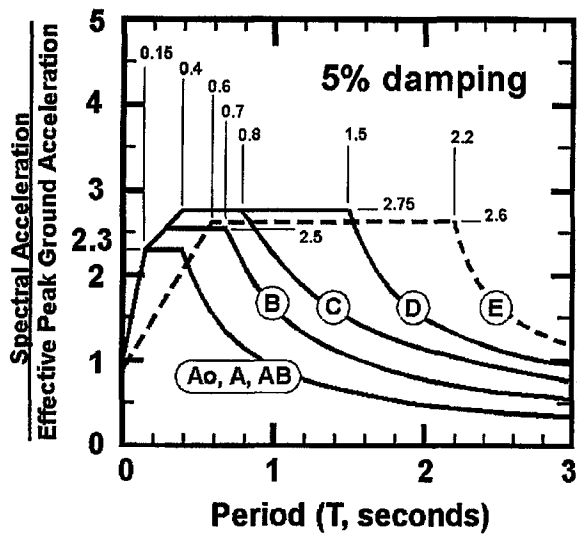

Fig. 31: Proposed Site Dependent Response Spectra with 5% Damping (Modified After Seed et al., 1997)
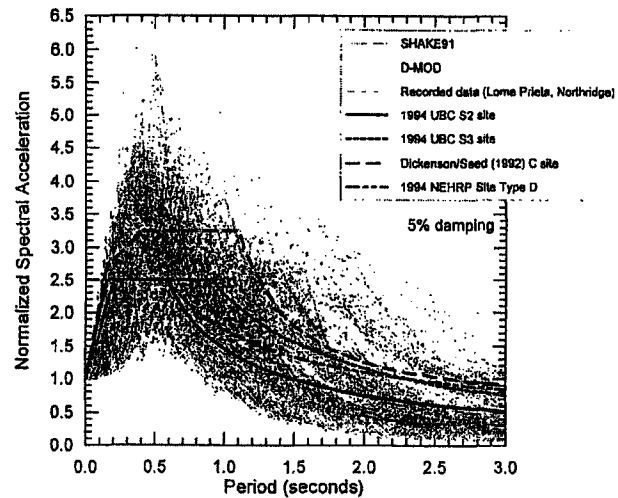

Fig. 33: Calculated Normalized Response Spectra for Oakland and Los Angeles Deep Stiff Sites Compared to Current Design Spectra (Chang et al., 1997)

where a_{max} is the expected peak ground surface acceleration. Larger degrees of period lengthening within this range are associated with the presence of soils that are particularly prone to reductions in stiffness at strong levels of shaking (e.g.: site classes C_4 through F in Table 3).

In lieu of performing site-specific site response analyses, improved approximate estimates of likely motions <u>at a specific site</u> can be made by "adding" an expected "peaking" of spectral response in the vicinity of T_p. Increasing spectral response, S_A (5% damped) at $T_{p,earthquake}$ by about 25%, and by about 20% at 0.95 and 1.05 $T_{p,earthquake}$, and then returning to unmodified S_A values at about 0.8 $T_{p,earthquake}$ and 1.15 $T_{p,earthquake}$ can provide improved representation of likely site motions <u>for a specific site</u>. This can be applied either to the types of empirical predictions presented in Table 3 and Figures 30 and 31, or to spectral shapes predicted by attenuation relationships developed based on "group averaging" of recorded strong motion data from "similar" sites.

Discussion of site response issues could be essentially an endless task, and this section could easily become as long as the treatment of soil liquefaction issues that dominates the beginning of this paper. Instead, we will truncate this discussion here and offer only the following (very brief) observations regarding key site response issues to be resolved over the next few years.

1. As increasingly responsible seismic design practice leads to consideration of higher levels of motion, especially in seismically active areas, and as "performance based design" calls for increasingly refined predictions of ground motions, there is a need to develop and further refine and validate improved modelling/analytical tools for fully nonlinear analysis of strong levels of shaking ($a_{max} > 0.3g$.). Higher levels of excitation are often strongly directional in nature, and cross-coupling of the different directions of motion calls for multi-directionally capable analytical tools and soil modeling capabilities.

2. Similarly, there is a need for improved understanding of the interactions between site response effects and near-field source mechanism and directionality effects (e.g. "pulse" and "fling"). As near-field motions are increasingly responsibly being addressed as a basis for design in seismically active regions, these important interactions involving directionally preferential and highly nonlinear response need to be better understood, and better and more reliable analytical modelling tools need to be calibrated and verified.

3. Geotechnical engineers need to better incorporate understanding of underlying seismological factors in assessing expected site response and ground motions for specific project sites. In addition to near-field source effects such as directionality and fling, basin response effects and regional "deep" structural effects are routinely poorly addressed in contemporary practice.

4. In addition to improvement of fully nonlinear modelling of multi-directional ground excitation, other areas in which progress is needed with respect to soil modelling include: (a) the need for better understanding and treatment of rate effects on the dynamic response characteristics of cohesive soils, and (b) improved understanding of the ramifications of the effects of soil softening and liquefaction (and also cyclic dilational "re-stiffening" of liquefiable soil types) on site response.

5. Variability of response of sites corresponding to site Classes AB_1 and AB_2 can be very high under strong levels of excitation. These can sometimes amplify very strong levels of excitation, and can produce very high levels of resultant surface motions in the near-field. Many current analytical models, and most current practice, do not yet adequately address this potentially dangerous condition which can arise at "Class AB" sites where a strong impedance contrast at the base of the soil or weathered rock zone can lead to entrapment of relatively high frequency energy and resultant resonant response.

6. Finally, improved treatment of soil-structure interaction, at high levels of excitation (and thus incorporating significant nonlinearity) is needed. A special sub-set here is the need for improved tools for both advanced (e.g.: finite element and/or finite difference) and "simplified" analysis and design treatment of seismic soil/pile/ superstructure interaction and performance.

SUMMARY AND CONCLUSIONS

There have been major advances in both seismic soil liquefaction engineering and in engineering assessment of seismic site response over the past decade. These advances have been spurred in no small part by lessons and data provided by earthquakes that have occurred since 1984. The advances achieved have, importantly, affected practice as well as research. Engineering treatment of site response issues has improved considerably, and soil liquefaction engineering has now grown into a semi-mature field in its own right.

As important and heartening as the recent advances in these two fields are, however, more needs to be done. Engineering treatment of seismic site response analysis needs to be better integrated with ongoing seismological advances, and improved treatments of (a) site response at very high levels of excitation ($a_{max} \geq 0.4g$.), (b) interactions of site effects with near-field effects (e.g.: "pulse" and "fling"), and (c) soil-structure interaction at high levels of excitation are needed. As engineers are increasingly asked to address higher levels of excitation, and as "performance-based design" begins to require increasingly detailed characterization of motions, the need for further advances will only increase. Fortunately, analytical methods are currently developing rapidly, and a wealth of recorded data from the recent Turkey and Taiwan

earthquakes, including some very important near-field strong motion recordings, offer significant promise here.

Similarly, recent seismic events provide both lessons and new questions in the area of soil liquefaction engineering. Major recent, and ongoing, advances are significantly improving our ability to predict the probability of "triggering" or initiation of soil liquefaction, but major gaps continue to persist with regard to our ability to accurately and reliable assess the likely consequences of liquefaction. This is particularly true for situations in which structural and/or site displacements and deformations are likely to be "small to moderate" ($\leq 0.7m.$). Improved analytical and design tools, and improved understanding of what constitutes "acceptable" performance, are urgently needed here.

The rapid rate of progress in both fields (site response assessment and liquefaction engineering) can be confidently expected to continue in the years ahead. Significant research efforts are currently underway to address all of these urgent needs. Over the next 3 to 5 years, engineers can expect to see the results of these efforts begin to make their way into practice.

In summary, the past decade has seen a laudable rate of improvements in practice, and more of the same can be expected with confidence over the next 3 to 5 years.

DEDICATION

We wish to dedicate this paper to Professor W. D. Liam Finn on this, the occasion of his "retirement", and in recognition of a lifetime spent pushing forward the frontiers of knowledge. On behalf of a profession that has learned so much as a result of his ebullient curiosity and keen intellect, we are deeply grateful.

REFERENCES

Andrews, D. C. A. and Martin, G. R. (2000) "Criteria for Liquefaction of Silty Soils." 12th World Conference on Earthquake Engineering, Proceedings, Auckland, New Zealand.

Andrus, R. D. (1994). "In situ characterization of gravelly soils that liquefied in the 1983 Borah Peak Earthquake." Ph.D. Dissertation, University of Texas at Austin.

Andrus, R.D. and Stokoe, K.H., (2000) "Liquefaction Resistance of Soils from Shear-Wave Velocity." Journal of Geotechnical and Geoenvironmental Engineering, Vol. 126, No. 11, pp. 1015-1025.

Arulanandan, K. and Symbico, J. (1993). "Post-liquefaction settlement of sands." Predictive soil mechanics : proceedings of the Wroth Memorial Symposium held at St. Catherine's College, Oxford, 27-29 July, Thomas Telford, London, p. 94-110.

Muraleetharan, K.K., Seed, R.B., Kabilamany, K. (1993). "Centrifuge Study of Volume Changes and Dynamic Stabilityof Earth Dams", J. Geotech. Engn., 119 (11), 1717-1731

Bartlett, S.F. and Youd, T.L. (1995) "Empirical Prediction Of Liquefaction-Induced Lateral Spreads," J. Geotech. Engng., ASCE, 121 (4), 316-329.

Boulanger, R. W. and Seed, R. B. (1995). "Liquefaction of Sand Under Bi-directional Monotonic and Cyclic Loading." Journal of Geotechnical Engineering, ASCE, 121(12), 870-878.

Cetin, K. O. and Seed, R. B. (2001a). "Nonlinear Shear Mass Participation Factor (r_d) for Cyclic Shear Stress Ratio Evaluation.", Submitted to the Journal of Geotechnical and Geoenvironmental Engineering.

Cetin, K. O. and Seed, R. B. (2001b). "Nonlinear Shear Mass Participation Factor (R_d) For Cyclic Shear Stress Ratio Evaluation", Research Report No. UCB/GT-2000/08, University of California, Berkeley.

Cetin, K. O., Seed, R. B., Der Kiureghian, A., Tokimatsu, K., Harder, L. F., and Kayen, R. E. (2000). "SPT-Based Probabilistic And Deterministic Assessment Of Seismic Soil Liquefaction Initiation Hazard", Research Report No. 2000/05, Pacific Earthquake Engineering Research Center.

Chang, W. S., Bray, J. D., Gookin, W. B., and Riemer, M. F. (1997). "Seismic Response Of Deep Stiff Soil Deposits in the Los Angeles, California Area During The 1994 Northridge, Earthquake.", Geotechnical Research Report No. UCB/GT/97-01, University of California, Berkeley.

Evans, M. D. (1987). "Undrained cyclic triaxial testing of gravels : the effect of membrane compliance." Ph.D. Thesis, University of California, Berkeley.

Evans, M. D. and Seed, H. B. (1987) "Undrained Cyclic Triaxial Testing Of Gravels : The Effect Of Membrane Compliance." Geotechnical Earthquake Engineering Research Report, Rep. No. UCB/EERC-87/08, University of California, Berkeley.

Finn, W. D. Liam. (1998) "Seismic Safety of Embankment Dams Development in Research and Practice 1988-1998." Geotechnical Special Publication No. 75, Proceedings of a Specialty Conference on Geotechnical Earthquake Engineering and Soil Dynamics III, pp. 812-853.

Finn, W. D. L., Ledbetter, R. H., and Wu, G. (1994) "Liquefaction in Silty Soils: Design and Analysis." Ground Failures under Seismic Conditions, Geotechnical Special

Publication 44, ASCE, New York, pp. 51-76.

France, J. W., Adams, T., Wilson, J., and Gillette, D. (2000). "Soil Dynamics and Liquefaction", Geotechnical Special Publication No. 107, ASCE.

Geyskens, P., Der Kiureghian, A., Monteiro, P. (1993), "Bayesian Updating of Model Parameters", Structural Engineering Mechanics and Materials Report No. UCB/SEMM-93/06, University of California at Berkeley.

Hamada, M., O'Rourke, T. D., and Yoshida, N. (1994). "Liquefaction-Induced Large Ground Displacement." Performance of Ground and Soil Structures during Earthquakes: Thirteenth International Conference on Soil Mechanics and Foundation Engineering, New Delhi, Proceedings, Japanese Society of Soil Mechanics and Foundation Engineering Pub., Tokyo, p. 93-108.

Hamada, M., Yasuda, S., Isoyama, R., and Emoto, K. (1986). "Study On Liquefaction Induced Permanent Ground Displacements", Report of the Association for the Development of Earthquake Prediction in Japan, Tokyo Japan, Available from the Faculty of Marine Science and Technology, Tokai University.

Harder, L. F. (1977). "Liquefaction of sand under irregular loading conditions." M.S. Thesis, University of California, Davis.

Harder, L. F. (1988). "Use of Penetration Tests to Determine the Cyclic Loading Resistance of Gravelly Soils During Earthquake Shaking." Ph.D. Thesis, University of California, Berkeley.

Harder, L. F. Jr. (1997) "Application of the Becker Penetration Test for Evaluating the Liquefaction Potential of Gravelly Soils." Proc., NCEER Workshop on Evaluation of Liquefaction Resistance of Soils, NCEER-97-0022.

Hausmann, M. R. (1990). Engineering principals of ground modification, McGraw Hill, pp. 632.

Hynes, M. E. (1988). "Pore pressure generation characteristics of gravel under undrained loading." Ph.D. Thesis, University of California, Berkeley.

Idriss, I. M. (2000), "Personal Communication"

Idriss, I. M., Sun, J. I., (1992), "Users Manual for SHAKE91, A Computer Program for Conducting Equivalent Linear Seismic Response Analyses of Horizontally Layered Soil Deposits, Program Modified Based on the Original SHAKE Program Published in December 1972, by Schnabel, Lysmer and Seed, August.

Ishihara, K. (1985). "Stability Of Natural Deposits During Earthquakes." 11th International Conference on Soil Mechanics and Foundation Engineering, Proceedings, San Francisco, v. 1, p. 321-376.

Ishihara, K. (1993). "Liquefaction And Flow Failure During Earthquakes: Thirty-Third Rankine Lecture," Geotechnique, 43(3), 351-415, London.

Ishimara, K. and Yoshimine, M. (1992) "Evaluation of Settlements in Sand Deposits Followiing Liquefaction During Earthquakes." Soils and Foundations, Vol. 32, No. 1, March, pp. 173-188.

Jong, H.-L. and Seed, R. B. (1988). "A Critical Investigation of Factors Affecting Seismic Pore Pressure Generation and Post-Liquefaction Flow Behavior of Saturated Soils", Geotechnical Engineering Research Report No. SU/GT/88-01, Stanford University.

Kishida, H. (1966), "Damage to Reinforced Concrete Buildings in Niigata City with Special Reference to Foundation Engineering", Soils and Foundations, Vol. VII, No. 1.

Koizumi, Y (1966), "Change in Density of Sand Subsoil caused by the Niigata Earthquake", Soils and Foundations, Vol. VIII, No. 2, pp. 38-44.

Liao, S. S. C., Lum, K. Y. (1998), "Statistical Analysis and Application of the Magnitude Scaling Factor in Liquefaction Analysis", Geotechnical Earthquake Engineering and Soil Dynamics III, Vol. 1, 410-421.

Liao, S. S. C., Veneziano, D., Whitman, R.V. (1988), "Regression Models for Evaluating Liquefaction Probability", Journal of Geotechnical Engineering, ASCE, Vol. 114, No. 4, pp. 389-409.

Liao, S. S. C., Whitman, R. V. (1986), "Overburden Correction Factor for SPT in Sand", Journal of Geotechnical Engineering, ASCE, Vol. 112, No. 3, March 1986, pp. 373-377.

Mitchell, J. K., Baxter, C. D. P., and Munson, T. C. (1995). "Performance of improved ground during earthquakes." Soil Improvement for Earthquake Hazard Mitigation, ASCE, New York, 1-36.

NCEER (1997), "Proceedings of the NCEER Workshop on Evaluation of Liquefaction Resistance of Soils", Edited by Youd, T. L., Idriss, I. M., Technical Report No. NCEER-97-0022, December 31, 1997.

Ohsaki, Y. (1966), "Niigata Earthquakes, 1964, Building Damage and Soil Conditions", Soils and Foundations, Vol. 6, No. 2, pp. 14-37.

Poulos, S. J., Castro, G., and France, J. W. (1985). "Liquefaction Evaluation Procedure." Journal of Geotechnical Engineering, ASCE, 111(6), 772-792.

Riemer, M. F. (1992). "The effects of testing conditions on the constitutive behavior of loose, saturated sands under monotonic loading." Ph.D. Thesis, University of California, Berkeley.

Riemer, M. F., Seed, R. B., and Sadek, S. (1993). "The SRS/RFT Soil Evaluation Testing Program." University of California, Berkeley Geotechnical Report No. UCB/GT-93/01.

Riemer, M.F., Seed, R.B. (1997), "Factors Affecting Apparent Position of Steady-State Line", Journal of Geotechnical and Geoenvironmental Engineering, Vol 123, No. 3, March 1997, pp. 281.

Robertson, P. K. and Wride, C. E. (1998). "Evaluating Cyclic Liquefaction Potential Using The Cone Penetration Test." Canadian Geotechnical Journal, 35(3), 442-459.

Seed, H. B., Idriss, I. M. (1971), "Simplified Procedure for Evaluating Soil Liquefaction Potential", Journal of the Soil Mechanics and Foundations Division, ASCE, Vol. 97, No SM9, Proc. Paper 8371, September 1971, pp. 1249-1273.

Seed, H. B., Seed, R. B., Harder, L. F., and Jong, H. L. (1989). "Re-evaluation of the Slide in the Lower San Fernando dam in the 1971 San Fernando earthquake", Earthquake Engineering Research Center Report No. UCB/EERC-88/04, University of California, Berkeley.

Seed, H. B., Tokimatsu, K., Harder, L. F., and Chung, R. M. (1985). "Influence of SPT Procedures in soil liquefaction resistance evaluations." Journal of Geotechnical Engineering, ASCE, 111(12), 1425-1445.

Seed, H. B., Tokimatsu, K., Harder, L. F., Chung, R. M. (1984), "The Influence of SPT Procedures in Soil Liquefaction Resistance Evaluations", Earthquake Engineering Research Center Report No. UCB/EERC-84/15, University of California at Berkeley, October, 1984.

Seed, R. B. and Harder, L. F. (1990). "SPT-Based Analysis Of Cyclic Pore Pressure Generation And Undrained Residual Strength." H.B. Seed Memorial Symposium, Berkeley, Ca., BiTech Publishing, Ltd., v. 2, p. 351-376.

Seed, R. B., Chang, S. W., Dickenson, S. E., and Bray, J. D. (1997) "Site-Dependent Seismic Response Including Recent Strong Motion Data." Proc., Special Session on Earthquake Geotechnical Engineering, XIV International Conf. On Soil Mechanics and Foundtion Engineering, Hamburg, Germany, A. A. Balkema Publ., Sept. 6-12, pp. 125-134.

Seed, R. B., Cetin, K. O., Der Kiureghian, A., Tokimatsu, K., Harder, L. F. Jr., and Kayen, R. E. (2001) "SPT-Based Probabilistic and Deterministic Assessment of Seismic Soil Liquefaction Potential." Submitted to the ASCE Journal of Geotechnical and Geoenvironmental Engineering.

Shamoto, Y., Zhang, J.-M., and Tokimatsu, K. (1998). "Methods for evaluating residual post-liquefaction ground settlement and horizontal displacement." Soils and Foundations, Special Issue, 69-83.

Stark, T. D. and Mesri, G. (1992). "Undrained Shear Strength of Liquefied Sands For Stability Analysis." Journal of Geotechnical Engineering, ASCE, 118(11), 1727-1747.

Toprak, S., Holzer, T. L., Bennett, M. J., Tinsley, J. C. (1999), "CPT- and SPT-based Probabilistic Assessment of Liquefaction Potential, Proceedings of Seventh U.S.-Japan Workshop on Earthquake Resistant Design of Lifeline Facilities and Countermeasures Against Liquefaction.

Vaid, Y.P., Chung, E.K.F., and Kuerbis, R.H. (1990). "Stress path and steady state." Canadian Geotechnical Journal, 27, 1-7.

Von Thun, J. L. (1986). "Analysis of Dynamic Compaction Foundation Treatment Requirements, Stage I, Jackson Lake Dam", Technical Memo No. TM-JL-230-26, Bureau of Reclamation, Engineering and Research Center, Embankment Dams Branch.

Yoshimi, Y., Tokimatsu, K., Ohara, J. (1994), "In-situ Liquefaction Resistance of Clean Sands Over a Wide Density Range", Geotechnique, Vol. 44, No. 3, pp. 479-494.

Youd, T. L., Idriss, I. M., Andrus, R. D., Arango, I., Castro, G., Christian, J. T., Dobry, R., Finn, W. D. L., Harder, L. F. Jr., Hynes, M. E., Ishihara, K., Koester, J. P., Liao, S. S. C., Marcuson, W. F. III., Martin, G, R., Mitchell, J. K., Moriwaki, Y., Power, M. S., Robertson, P. K., Seed, R. B., and Stokoe, K. H., II. (1997) Summary Paper, Proc., NCEER Workshop on Evaluation of Liquefaction Resistance of Soils, NCEER-97-0022.

Youd, T. L. (2000) Personal Communication.

Youd et al. (2001) Personal Communication.

Youd, T. L., Noble, S. K. (1997), "Liquefaction Criteria Based on Statistical and Probabilistic Analyses", Proceedings of the NCEER Workshop on Evaluation of Liquefaction Resistance of Soils, December 31, 1997, pp. 201-205.